arXiv:1511.05073v1 [cs.IT] 16 Nov 2015

Analysis of Massive MIMO-Enabled Downlink Wireless Backhauling for Full-Duplex Small Cells

Hina Tabassum, Ahmed Hamdi Sakr, and Ekram Hossain

***Abstract*—Recent advancements in self-interference (SI) cancellation capability of low-power wireless devices motivate in-band full-duplex (FD) wireless backhauling in small cell networks (SCNs). In-band FD wireless backhauling allows the use of same frequency spectrum for the backhaul as well as access links of the small cells concurrently. In this paper, using tools from stochastic geometry, we develop a framework to model the downlink rate coverage probability of a user in a given SCN with massive MIMO-enabled wireless backhauls. The considered SCN is composed of a mixture of small cells that are configured in either in-band or out-of-band backhaul modes with a certain probability. The performance of the user in the considered hierarchical network is limited by several sources of interference such as the backhaul interference, small cell base station (SBS)-to-SBS interference and the SI. Moreover, due to the channel hardening effect in massive MIMO, the backhaul links experience long term channel effects only, whereas the access links experience both the long term and short term channel effects. Consequently, the developed framework is flexible to characterize different sources of interference while capturing the heterogeneity of the access and backhaul channels. In specific scenarios, the framework enables deriving closed-form coverage probability expressions. Under perfect backhaul coverage, the simplified expressions are utilized to optimize the proportion of in-band and out-of-band small cells in the SCN in closed-form. Finally, few remedial solutions are proposed that can potentially mitigate the backhaul interference and in turn improve the performance of in-band FD wireless backhauling. Numerical results investigate the scenarios in which in-band wireless backhauling is useful and demonstrate that maintaining a correct proportion of in-band and out-of-band FD small cells is crucial in wireless backhauled SCNs.**

***Index Terms*—5G cellular, small cells, massive MIMO, full-duplex, self-interference, self-backhauling, stochastic geometry, backhaul interference.**

I. Introduction

Massive deployment of small cells will be a key feature of the emerging 5G cellular networks [1]. Subsequently, efficient forwarding of the backhaul traffic of the small cells will be a key challenge. By definition, the small cell backhaul connections are used to (i) forward/receive the end-user (small cell user) data to/from the core network and (ii) exchange mutual information among different small cells. Typically, the backhaul of small cells exploits either wired connectivity (e.g., optical fiber and DSL connections) or wireless connectivity (e.g., microwave or millimeter wave [mmwave] links). However, the prohibitively high cost of wired connectivity, directed transmission requirement of the microwave links, and the poor penetration of the mmwave links make them less attractive backhaul solutions. To this end, leveraging the use of radio access network (RAN) spectrum simultaneously for both access and backhaul links has emerged as a potential backhaul solution [2], [3]. Backhauling based on RAN spectrum exhibits less-sensitivity to channel propagation effects, provide wider coverage due to non-LOS propagation, makes the reuse of existing hardware possible, and thus enable simpler operation and maintenance (O&M). Nonetheless, the RAN spectrum availability is quite limited.

To enable efficient use in the RAN spectrum, full-duplex (FD) transmission has been recently considered as a viable solution for 5G networks. FD transmission implies simultaneous transmission and reception of information in the same frequency band. FD transmission can be realized at base stations (BSs) through two different antenna configurations, i.e., shared and separated antenna configurations [4]. The shared antenna configuration uses a single antenna for simultaneous in-band transmission and reception through a three-port circulator. On the other hand, the separated antenna configuration requires separate antennas for transmission and reception. The gains of FD transmission are however limited by the overwhelming nature of self-interference (SI), which is generated by the transmitter to its own collocated receiver [5]. Fortunately, with the recently developed antenna and digital baseband technologies, SI can be reduced close to the level of noise floor in low-power devices [6]. As such, FD transmission in the access and backhaul links of small cells enables reuse of RAN spectrum, alleviates the need to procure spectrum for backhauling, and facilitates hardware implementation.

A. Background Work

Several recent studies focus on developing backhaul interference management schemes [7], [8] and backhaul delay minimizing solutions [9]. In [7], an interference management strategy is proposed for self-organized small cells. The small cell base stations (SBSs) operate like decode-and-forward relays for the macrocell users and forward their uplink traffic to the macrocell base station (MBS) over heterogeneous backhauls. The problem is formulated as a non-cooperative game and a reinforcement learning approach is used to find an equilibrium. In [8], a duplex and spectrum sharing scheme based on co-channel reverse time-division duplex (TDD) and dynamic soft frequency reuse (SFR), are proposed for backhaul interference management. An optimization problem is formulated to allocate backhaul bandwidth and to optimize user association such that the network sum-rate is maximized. A tractable model is developed in [9] to characterize the backhaul delay experienced by a typical user in the downlink considering both wired and wireless backhauls. It is shown that deploying dense small cell networks may not be effective without a comparable investment in the backhaul network.

The work was supported by the Natural Sciences and Engineering Research Council of Canada (NSERC).

Along another line of research, the performance gains of FD SBSs are recently analyzed for concurrent uplink and downlink transmissions in various research studies considering a single antenna [10]–[14] and multi-antenna [15], [16] transmissions. In [10], the feasibility conditions of FD operation are investigated followed by developing an uplink/downlink user scheduling scheme that maximizes the overall utility of all users. In [11], a resource management scheme is developed that assigns downlink and uplink transmissions jointly and perform mode selection at each resource block while considering the gain of SI cancellation. Users' transmit power levels are then determined such that the total utility sum is maximized. Another optimization-based study considers maximizing the sum-rate performance by jointly optimizing subcarrier assignment and power allocation considering FD transmissions [12].

In [13], considering Rayleigh fading channels and ideal backhauls for SBSs, a downlink throughput analysis of a K-tier network is conducted in which the SBSs operate in either a downlink half-duplex (HD) or a bi-directional FD[1] mode. It is shown that all BSs should operate in either HD or FD mode to maximize network throughput. Using Wyner model, [14] analyzes the network rate under single-cell processing and cloud-RAN operation considering either HD or FD BSs. Insights are extracted related to the regimes in which FD BSs are advantageous. In [15], the gains of using multiple-antennas for HD multiple-input-multiple-output (MIMO) link are compared to the gain achieved by utilizing the antennas for FD transmission. Conditions are analyzed in which using additional antennas for FD transmission is beneficial instead of high capacity HD MIMO link. For a single massive MIMO-enabled MBS and small cells deployed on a fixed distance from the MBS (ignoring the co-tier interference among SBSs), a precoding method is designed in [16]. The precoding method enables complete rejection of backhaul interference received at a given user from the MBS to which the serving SBS of that user is associated with.

B. Motivation and Contributions

Although the feasibility of HD SBSs (referred as out-of-band FD SBSs in this paper) has been investigated for wireless backhauls, there has not been any comprehensive study on the performance and feasibility of FD SBSs (referred as in-band FD SBSs in this paper) in wireless backhauled small cell networks. While the in-band FD operation can ideally double the spectral efficiency in a link, the network-level gain of exploiting FD transmission in the wireless backhauls remains unclear due to the complicated interference environments, e.g., SI, co-tier, and cross-tier interferences at the backhaul and access links (as illustrated in Fig. 1). Therefore, the use of in-band backhauling is not immediately evident over the popular out-of-band backhauling. A theoretic framework is required to characterize the diverse interference issues and to critically analyze the scenarios in which in-band backhauling may be beneficial over out-of-band backhauling. In this context, the contributions of this paper are listed as follows:

- Using tools from stochastic geometry, we model the performance of a massive MIMO-enabled wireless backhaul network that supports single-antenna small cells. A hierarchical network structure is considered in which the massive MIMO-enabled wireless backhaul hubs (or connector nodes (CNs)) are deployed to provide simultaneous backhaul to multiple SBSs. Each SBS can be configured either in the in-band or out-of-band FD backhaul mode with a certain probability. Note that the in-band FD backhaul mode leads to three-node full-duplex (TNFD) transmission which involves three nodes, i.e., the CN transmits to an SBS and the SBS transmits to a user[2].
- The downlink rate coverage (which is a function of the rate coverage in the access and backhaul links) of a small cell user is derived considering both the in-band and out-of-band FD backhaul modes of a given SBS. Due to the channel hardening effect in massive MIMO, the backhaul links experience long-term channel effects only, whereas the access links experience both the long term and short term channel effects. Thus, unlike traditional Rayleigh fading assumption, the framework captures the heterogeneity of the access and backhaul links.
- Closed-form rate coverage expressions are then provided for specific scenarios. The simplified expressions, under the assumption of perfect backhaul coverage, are then utilized to customize the proportion of in-band and out-of-band FD SBSs in a small cell network in closed-form.
- A distributed backhaul interference-aware mode selection mechanism is then discussed to gain insights into selecting the proportion of in-band and out-of-band FD SBSs as a function of network parameters.
- Due to backhaul interference, downlink transmission to a user by an SBS is directly affected by the transmission in the backhaul link to this SBS. We therefore present few remedial solutions that can potentially mitigate the backhaul interference and quantify the enhancements in the performance of in-band FD wireless backhauls.

Numerical results demonstrate the usefulness of in-band FD wireless backhauls in scenarios with low SI, low transmit power and intensity of CNs, and higher intensity of SBSs. It is also shown that solely implementing the in-band or out-of-band FD backhaul solutions may not be useful. Instead, a system with the correct proportion of in-band and out-of-band FD SBSs should be implemented.

C. Paper Organization and Notations

The rest of the paper is structured as follows. Section II discusses the system model and assumptions, the channel model, and the massive MIMO-enabled wireless backhaul model. Section III formulates the signal-to-interference-plus-noise ratio (SINR) model, performance metrics, and discusses

[1]Bi-directional FD mode allows both the transmitter and the receiver to transmit signals to each other at the same time and in the same frequency band.

[2]Interested readers are referred to [5] for the details of TNFD mode of transmission. In the TNFD mode, a typical user suffers from backhaul interference (i.e., the interference received at a typical user from the CN which is associated to its designated in-band FD SBS).

some of the approximations considered throughout the paper. Section IV derives the rate coverage expressions for a given SBS considering both in-band and out-of-band FD backhaul modes. Section V provides the simplified rate coverage expressions and customizes the proportion of in-band and out-of-band FD SBSs in the network. Backhaul interference management techniques are discussed in Section VI. Section VII provides numerical and simulation results followed by the concluding remarks in Section VIII.

Notation: $\mathrm{Gamma}(k_{(\cdot)}, \theta_{(\cdot)})$ represents a Gamma distribution with shape parameter k, scale parameter θ and $(\cdot)$ displays the name of the random variable (RV). $\Gamma(a) = \int_0^\infty x^{a-1}e^{-x}dx$ represents the Gamma function, $\Gamma_u(a;b) = \int_b^\infty x^{a-1}e^{-x}dx$ denotes the upper incomplete Gamma function, and $\Gamma_l(a;b) = \int_0^b x^{a-1}e^{-x}dx$ denotes the lower incomplete Gamma function [17]. ${}_2F_1[\cdot,\cdot,\cdot]$ denotes the Gauss Hypergeometric function and $\mathcal{B}(\cdot,\cdot,\cdot)$ denotes the incomplete Beta function. $f(\cdot)$ and $F(\cdot)$ denote the probability density function (PDF) and cumulative distribution function (CDF), respectively. Finally, $\mathbb{E}[\cdot]$ denotes the expectation operator.

II. System Model and Assumptions

A. Network Deployment Model

We consider a downlink two-tier cellular network with small cells connected to the core network through connector nodes (CNs). The CNs provide wireless backhaul connections to the small cells. A CN is typically situated at a fiber point-of-presence or where high-capacity line-of-sight (LOS) microwave link is available to the core network. An existing MBS can be an example of such a CN which is connected to the core network by fiber-to-the-cell (FTTC) links. The locations of the CNs, SBSs, and users are modeled according to independent homogeneous Poisson Point Processes (PPPs) Φ'_{c}, Φ'_{s}, and Φ'_{u} with intensities λ'_c, λ'_s, and λ'_u, respectively. Specifically, for a given PPP, the number of points and their locations are random and they follow Poisson and uniform distributions, respectively. The abstraction model where the nodes are distributed using PPP has been shown to be quite effective for system-level performance evaluation of cellular networks (see [18] and references therein)[3]. For the downlink transmission, each user (and SBS) associates to the SBS (and CN) that offers the strongest average received power.

B. Channel Model

Throughout the paper, the propagation channels related to network elements of the same type are assumed to be independent and identically distributed (i.i.d.). If a generic CN-to-SBS link is considered, e.g., from the CN i to the SBS k, the channel parameters are identified by using the subscript $\{\mathrm{c_i}, \mathrm{s_k}\}$. A similar notation holds for the channel parameters related to other network elements. The wireless channels are subject to path-loss, shadowing, and fast-fading.

[3]Other modeling options may also be used, e.g., the locations of the CNs might be correlated with the SBSs. This can be taken into account by considering non-Poisson point processes. However, for analytical intractability, such a modeling option is not considered in this paper.

1) Path-Loss: Let r_{X_i,Y_k} be the distance between two generic network elements X_i and Y_k. Based on the downlink network model, we have $X_i \in \{\mathrm{c}_i, \mathrm{s}_i\}$ and $Y_k \in \{\mathrm{s}_k, \mathrm{u}_k\}$ where c, s, and u denote the generic CN, SBS, and user, respectively. The path-loss of this generic link is defined as $r_{X,Y}^{-\beta}$ (for ease of exposition, we exclude the subscripts of X and Y) where $\beta > 2$ denotes the path-loss exponent.

2) Shadowing and Fading: In addition to the distance-dependent path-loss, the generic link is subject to both the shadowing $S_{X,Y}$ and fast fading $F_{X,Y}$, unless stated otherwise. We model shadowing with the log-normal distribution where $\mu_{X,Y}$ and $\sigma_{X,Y}$ are the mean and standard deviation of the shadowing channel power, respectively. Furthermore, the fading component of the wireless channel is modeled by the Nakagami-*m* distribution. Nakagami-*m* is a generic fading distribution which includes Rayleigh distribution for $m = 1$ (typically used for non-LOS conditions) as a special case and can well-approximate the Rician fading distribution for $1 \leq m \leq \infty$ (typically used for strong LOS conditions) [19].

Remark 1 (Displacement Theorem [20])**.** The displacement theorem can be used to deal with the shadow fading $S_{X,Y}$ as a random and independent transformation of a given homogeneous PPP Φ of density λ. In this case, the resulting point process is also a PPP with equivalent density $\lambda\mathbb{E}[S_{X,Y}^{\frac{2}{\beta}}]$. Applying this theorem to our case, we can handle the effect of any distribution for the shadow fading as long as the fractional moment $\mathbb{E}[S_{X,Y}^{\frac{2}{\beta}}]$ is finite. For log-normal shadowing, the fractional moment can be given by using the definition of its moment generating function (MGF) as follows:

$$\mathbb{E}[S_{X,Y}^{\frac{2}{\beta}}] = \exp\left(2\frac{\mu_{X,Y}}{\beta} + 0.5\left(2\frac{\sigma_{X,Y}}{\beta}\right)^2\right). \quad (1)$$

As such, Φ'_c and Φ'_s become Φ_c and Φ_s with densities $\lambda_c = \lambda'_c\mathbb{E}[S_{X,Y}^{\frac{2}{\beta}}]$ and $\lambda_s = \lambda'_s\mathbb{E}[S_{X,Y}^{\frac{2}{\beta}}]$, respectively. Thus, a generic useful or interfering link gain given by $r_{X,Y}^{-\beta}S_{X,Y}F_{X,Y}$, where r follows a PPP Φ', will be modeled as $r_{X,Y}^{-\beta}F_{X,Y}$ where r follows a PPP Φ throughout the paper.

C. Backhaul Modes of Operation at SBSs

Each SBS can operate in two modes for backhaul transmission, i.e.,

- *In-band full-duplex (IBFD) mode:* in which the access link and backhaul link transmissions are conducted simultaneously at the same frequency band (i.e., F_1 in Fig. 1).
- *Out-of-band full-duplex (OBFD) mode:* in which the access link and backhaul link transmissions are conducted in orthogonal channels, i.e., access link transmissions take place at frequency band F_2 while the backhaul link transmissions take place at frequency band F_1 simultaneously. Both F_1 and F_2 are assumed to have same bandwidth.

For efficient antenna usage, in this paper, FD operation is achieved at the SBS using a shared antenna that separates the transmitting and receiving circuit chains through an ideal circulator. The transmission mode selection for small cells is modeled by independent Bernoulli RVs such that small cells are configured in IBFD and OBFD mode with probability q

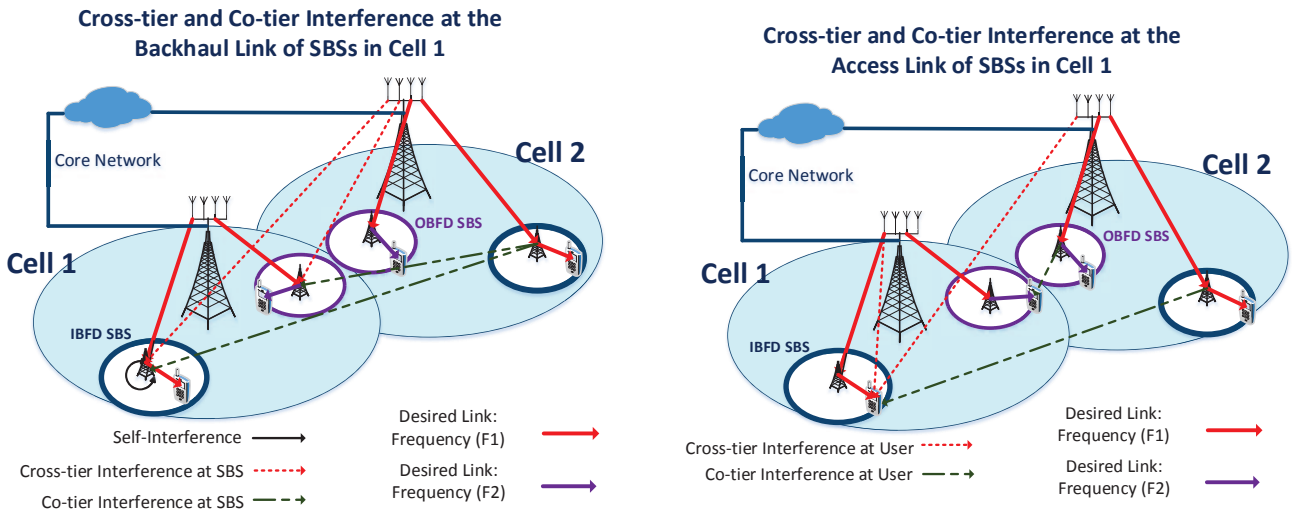

Fig. 1: Graphical illustration of the considered massive MIMO-enabled wireless backhaul network for both in-band and out-of-band small cells. Co-tier and cross-tier interferences experienced at the access and backhaul links are illustrated for in-band and out-of-band small cells located in cell 1.

and $1-q$, respectively, where q is identical for all small cells. With the independent thinning of $\Phi_{\rm s}$, we can represent the SBSs in IBFD and OBFD modes as two independent PPPs $\Phi_{\rm sI}$ and $\Phi_{\rm sO}$ with density $q\lambda_s$ and $(1-q)\lambda_s$, respectively.

D. Massive MIMO-enabled Backhaul Model

Each CN is equipped with M antennas that serves the backhaul links of a maximum of $\mathcal{S}$ single-antenna SBSs. Each SBS serves one user at a time and each user device is equipped with one antenna. We refer to the massive MIMO regime as the case where $1 \ll \mathcal{S} \ll M$. During the training phase, each SBS sends a pre-assigned orthogonal pilot sequence to the CN which is estimated perfectly by the CN and the pilot sequence is not used by any other CN (i.e., no pilot contamination is assumed)[4]. The channel estimation is facilitated by considering time division duplexing (TDD) at CNs such that the channel reciprocity is guaranteed. The maximum number of downlink backhaul data streams $\mathcal{S}$ per CN depends on the dimension of the uplink pilot field, which in turn determines the number of channel vectors that can be estimated and for which the downlink precoder can be calculated.

Each CN serves its SBSs by using linear zero-forcing beamforming (LZFBF) with equal power per backhaul data stream. As such, in the massive MIMO regime, the effects of Gaussian noise and uncorrelated intra-cell interference disappear. The rates of backhaul links to different SBSs thus tend to concentrate on deterministic limits that are calculated using tools from asymptotic random matrix theory. In this paper, we use the following formula for the backhaul data rate in the link between a CN and a given SBS [21]:

$$R_b = \alpha \log_2\left(1+\frac{M-\min(\mathcal{N}_s,\mathcal{S})+1}{\min(\mathcal{N}_s,\mathcal{S})}\mathrm{SIR}_b\right), \quad (2)$$

[4]Some guidelines will be provided in Section VII on how to incorporate the effect of interference due to pilot contamination.

where $\mathcal{N}_s$ denotes the number of SBSs associated with the CN, $\min(\mathcal{N}_s,\mathcal{S})$ is the number of SBSs served by the CN at a time, the factor in the numerator $M-\min(\mathcal{N}_s,\mathcal{S})+1$ is the massive MIMO gain, the factor $\min(\mathcal{N}_s,\mathcal{S})$ in the denominator is due to dividing the CN's transmit power equally per backhaul stream in the useful link, and SIR_b denotes the signal-to-interference ratio (SIR) at the SBS (with some abuse of the notation due to the multiplying factor $\frac{M-\min(\mathcal{N}_s,\mathcal{S})+1}{\min(\mathcal{N}_s,\mathcal{S})}$), and α is the *backhaul access probability* of a given SBS, which is defined as the probability that an SBS is served by a CN over a backhaul link. Without loss of generality, we ignore the impact of the time required for channel estimation in (2); however, it can be incorporated by multiplying R_b with the ratio of time spent sending data to the total time frame [22].

E. Load of CNs and Backhaul Access Probability of SBSs

Note that the number of SBSs $\mathcal{N}_s$ associated to a given CN using the strongest signal association policy is a RV and can exceed the supported number of backhaul streams $\mathcal{S}$. The probability mass function (PMF) of the number of SBSs served by a generic CN can be given as follows [23]:

$$\mathbb{P}(\mathcal{N}_s=n)=\frac{b^b\Gamma(n+b)(\mathbb{E}[\mathcal{N}_s])^n}{\Gamma(n+1)\Gamma(b)(b+\mathbb{E}[\mathcal{N}_s])^{n+b}}, \quad (3)$$

where $\mathbb{E}[\mathcal{N}_s]=\lambda_s/\lambda_c$ is the average number of SBSs per CN. This expression is derived by approximating the area of a Voronoi cell by a gamma-distributed RV with shape parameter $b=3.575$ and scale parameter $\frac{1}{b\lambda_c}$. Note that this expression is valid only when the SBSs are assumed to be spatially distributed according to an independent PPP.

In case when all SBSs associated to a given CN cannot be served at the same time, the CN randomly picks a set of $\mathcal{S}$ SBSs. The backhaul access probability of an SBS can thus be

derived as follows:

$$\alpha = \begin{cases} 1, & \mathcal{N}_s \leq \mathcal{S} \\ \frac{\binom{\mathcal{N}_s-1}{\mathcal{S}-1}}{\binom{\mathcal{N}_s}{\mathcal{S}}} = \frac{\mathcal{S}}{\mathcal{N}_s}, & \mathcal{N}_s > \mathcal{S} \end{cases} = \min\left(1, \frac{\mathcal{S}}{\mathcal{N}_s}\right). \quad (4)$$

III. Performance Metrics and SINR Model of IBFD and OBFD Transmission Modes

In this section, we define the performance metrics of interest, characterize the different sources of interference, and formulate the SINR at the access and backhaul links of the SBSs in both the IBFD and OBFD modes of backhaul operation. Some relevant remarks regarding the intensity of interfering sources and approximations are also highlighted which will be applied for the analytical evaluation of the rate coverage probability expressions later in Section IV.

A. Performance Metrics

Generally speaking, the downlink SINR coverage probability of a given SBS is defined as the probability with which its user's SINR exceeds a predefined SINR target. Nevertheless, due to the difference in the number of frequency resources required for IBFD and OBFD mode, the rate of a given SBS becomes a more relevant performance metric.

The instantaneous downlink rates at the access link of a given SBS in the IBFD and OBFD modes are defined, respectively, as:

$$\begin{aligned} \mathcal{R}_{\mathrm{a,I}} =& \log_2(1+\mathrm{SINR}_{\mathrm{a,I}}), \\ \mathcal{R}_{\mathrm{a,O}} =& \frac{1}{2}\log_2(1+\mathrm{SINR}_{\mathrm{a,O}}). \end{aligned} \quad (5)$$

The instantaneous downlink rates at the backhaul link of a given SBS in the IBFD and OBFD modes are defined using (2), respectively, as follows:

$$\begin{aligned} \mathcal{R}_{\mathrm{b,I}} =& \alpha \log_2\left(1+\frac{M-\min(\mathcal{N}_s,\mathcal{S})+1}{\min(\mathcal{N}_s,\mathcal{S})}\ \mathrm{SIR}_{\mathrm{b,I}}\right), \\ \mathcal{R}_{\mathrm{b,O}} =& \frac{\alpha}{2}\log_2\left(1+\frac{M-\min(\mathcal{N}_s,\mathcal{S})+1}{\min(\mathcal{N}_s,\mathcal{S})}\ \mathrm{SIR}_{\mathrm{b,O}}\right). \end{aligned} \quad (6)$$

Note that the factor of $\frac{1}{2}$ appears in the rates of the OBFD case (i.e., $\mathcal{R}_{\mathrm{a,O}}$ and $\mathcal{R}_{\mathrm{b,O}}$) since two different frequency bands are used by the SBSs (to receive in the backhaul link and transmit in the access link) in the out-of-band backhaul mode. In the IBFD mode, the SBSs use only one frequency band.

1) Downlink rate coverage of an SBS in IBFD mode: Now let us define the rate coverage probability $\mathcal{C}_I$ of a given SBS operating in IBFD mode as the probability that the downlink user rate is higher than a required target rate R_{th}. To achieve R_{th} in IBFD mode, both $\mathcal{R}_{\mathrm{b,I}}$ and $\mathcal{R}_{\mathrm{a,I}}$ must be at least R_{th}. In other words, $\mathrm{SINR}_{\mathrm{a,I}}$ must be greater than a prescribed threshold $\gamma_{\mathrm{a,I}}$ to achieve a target rate of R_{th} in the access link, where $\gamma_{\mathrm{a,I}}$ can be given using (5) as follows:

$$\gamma_{\mathrm{a,I}} = 2^{R_{\mathrm{th}}} - 1. \quad (7)$$

On the other hand, $\mathrm{SIR}_{\mathrm{b,I}}$ must be greater than another prescribed threshold $\gamma_{\mathrm{b,I}}$ to achieve a target rate of R_{th} in the backhaul link. Using (6), $\gamma_{\mathrm{b,I}}$ can be defined as follows:

$$\gamma_{\mathrm{b,I}} = \frac{\min(\mathcal{N}_s,\mathcal{S})}{M-\min(\mathcal{N}_s,\mathcal{S})+1}\left(2^{\frac{R_{\mathrm{th}}}{\alpha}}-1\right). \quad (8)$$

The coverage probability $\mathcal{C}_{\mathrm{I}}$ of an SBS in the IBFD mode is a function of the SINR at both the access link and the backhaul link, and the SINR outage probability $\mathcal{C}_{\mathrm{I}}$ is defined as follows:

$$\mathcal{C}_{\mathrm{I}} = \mathbb{P}(\mathrm{SIR}_{\mathrm{b,I}} > \gamma_{\mathrm{b,I}})\ \mathbb{P}(\mathrm{SINR}_{\mathrm{a,I}} > \gamma_{\mathrm{a,I}}). \quad (9)$$

2) Downlink rate coverage of an SBS in OBFD mode: The rate coverage probability of an SBS in the OBFD mode is given as

$$\mathcal{C}_{\mathrm{O}} = \mathbb{P}(\mathrm{SIR}_{\mathrm{b,O}} > \gamma_{\mathrm{b,O}})\ \mathbb{P}(\mathrm{SINR}_{\mathrm{a,O}} > \gamma_{\mathrm{a,O}}), \quad (10)$$

where $\gamma_{\mathrm{a,O}} = 2^{2R_{\mathrm{th}}} - 1$ from (5). To achieve R_{th} in the backhaul link, $\gamma_{\mathrm{b,O}}$ can be defined from (6) as follows:

$$\gamma_{\mathrm{b,O}} = \frac{\min(\mathcal{N}_s,\mathcal{S})}{M-\min(\mathcal{N}_s,\mathcal{S})+1}\left(2^{\frac{2R_{\mathrm{th}}}{\alpha}}-1\right). \quad (11)$$

3) Downlink rate coverage of a typical user: The overall rate coverage probability of a typical user depends on the probability of a given SBS to operate in OBFD or IBFD mode and can thus be given as

$$\mathcal{C}_u = q\mathcal{C}_{\mathrm{I}} + (1-q)\mathcal{C}_{\mathrm{O}}. \quad (12)$$

B. SINR Model for IBFD Mode

1) Access link: The SINR of a generic user associated with an SBS in the IBFD mode can be defined as follows:

$$\mathrm{SINR}_{\mathrm{a,I}} = \frac{P_s\ F_{\mathrm{s,u}}\ r_{\mathrm{s,u}}^{-\beta}}{I_{\mathrm{s,u}} + I_{\mathrm{c,u}} + N_0}, \quad (13)$$

where P_s denotes the transmit power of a generic SBS, $r_{\mathrm{s,u}}$ and $F_{\mathrm{s,u}}$ denote the distance and the Gamma distributed fading between a user and its serving SBS, respectively, and N_0 is the thermal noise power. Since Φ_{s} is a stationary PPP, the PDF of the distance $r_{\mathrm{s,u}}$ is given by the Rayleigh distribution, i.e., $f_{r_{\mathrm{s,u}}}(r) = 2\pi\lambda_s r e^{-\pi\lambda_s r^2}$.

In the IBFD mode, a given user experiences interference from all SBSs in IBFD mode which receive backhaul data from their corresponding CN. Thus, $I_{\mathrm{s,u}}$ can be modeled as follows:

$$I_{\mathrm{s,u}} = \sum_{x\in\bar{\Phi}_{\mathrm{sI}}\setminus\mathrm{s}} P_s\ F_{\mathrm{x,u}}\ r_{\mathrm{x,u}}^{-\beta}, \quad (14)$$

where $\bar{\Phi}_{\mathrm{sI}}$ denotes the PPP of successfully backhauled SBSs in IBFD mode with intensity $\bar{\lambda}_{\mathrm{sI}}$ and can be given using the **mean load approximation** and **Remark 2** detailed below.

Mean load approximation: For analytical tractability, we approximate the number of SBSs $\mathcal{N}_s$ associated to a given CN by its average value, i.e., $\mathbb{E}[\mathcal{N}_s] = \lambda_s/\lambda_c$. As such, the average number of SBSs in IBFD mode served per CN can be given by $q\min(\lambda_s/\lambda_c, \mathcal{S})$.

Remark 2 (Intensity of Interfering SBSs in IBFD Mode)**.** Given the average number of SBSs in IBFD mode served per CN, the intensity $\bar{\lambda}_{\mathrm{sI}}$ of the interfering SBSs in IBFD mode can be defined as $q\min(\lambda_s/\lambda_c, \mathcal{S})\,\lambda_c$. The impact of the **mean**

load approximation will be demonstrated through numerical results in Section VII.

The interference at a user due to backhaul transmissions can be modeled as follows:

$$I_{\mathrm{c,u}} = \sum_{y \in \Phi_c} P_c \, r_{\mathrm{y,u}}^{-\beta}, \tag{15}$$

Note that the interference at a user will be received from all streams of a given CN thus the total interfering power from a CN is P_c and there is no short-term fading factor in the interference experienced from the CNs due to the channel hardening effect.

2) Backhaul link: The received SIR on the backhaul link of a given SBS in IBFD mode is given as:

$$\mathrm{SIR}_{\mathrm{b,I}} = \frac{P_c \, r_{\mathrm{c,s}}^{-\beta}}{I_{\mathrm{s,s}} + I_{\mathrm{c,s}} + I_{\mathrm{SI}}}, \tag{16}$$

where $r_{\mathrm{c,s}}$ denotes the distance between the SBS and its serving CN c. Note that the impact of equal power allocation per backhaul stream (i.e., the denominator of CN's transmit power $\frac{P_c}{\min(\mathcal{N}_s, \mathcal{S})}$) has already been incorporated in the desired SIR threshold $\gamma_{\mathrm{b,I}}$ (see (2) and (8)). Therefore it is not considered in (16). Since Φ_c is stationary PPP, the PDF of the distance $r_{\mathrm{c,s}}$ between each CN and its designated SBS is given by the Rayleigh distribution, i.e., $f_{r_{\mathrm{c,s}}}(r) = 2\pi\lambda_c r e^{-\pi\lambda_c r^2}$.

Since the SI incurred at a given SBS in IBFD mode depends on its own transmit power, we can define the residual SI power after performing SI cancellation as follows:

$$I_{\mathrm{SI}} = \frac{P_s}{\xi}, \tag{17}$$

where ξ represents the SI cancellation capability of the SBS. Note that ξ depends on the nature of the SI cancellation algorithms. For ease of exposition, we consider ξ as a constant value in this paper.

In the backhaul, a given SBS in the IBFD mode experiences interference from all other SBSs operating in IBFD mode receiving their backhaul data from their corresponding CN. Thus $I_{\mathrm{s,s}}$ can be modeled as $I_{\mathrm{s,s}} = \sum_{x \in \bar{\Phi}_{\mathrm{sI}}} P_s \; F_{\mathrm{x,s}} \; r_{\mathrm{x,s}}^{-\beta}$, where $r_{\mathrm{x,s}}$ and $F_{\mathrm{x,s}}$ represent the distance and fast fading channel between the two SBSs operating in IBFD mode, respectively. Note that $\bar{\Phi}_{\mathrm{sI}}$ is defined by $\bar{\lambda}_{\mathrm{sI}}$ given in **Remark 2**. Finally, the interference received at an SBS from neighboring CNs can be modeled as $I_{\mathrm{c,s}} = \sum_{y \in \Phi_c \setminus \mathrm{c}} P_c r_{\mathrm{y,s}}^{-\beta}$.

C. SINR Model for OBFD SBS

1) Access link: The SINR received at a generic user associated to an SBS s operating in OBFD mode can be defined as follows:

$$\mathrm{SINR}_{\mathrm{a,O}} = \frac{P_s \; F_{\mathrm{s,u}} \; r_{\mathrm{s,u}}^{-\beta}}{\hat{I}_{\mathrm{s,u}} + N_0}, \tag{18}$$

where $\hat{I}_{\mathrm{s,u}}$ is the interference experienced by the user from all other SBSs operating in OBFD mode which are receiving their backhaul data from their corresponding CN, i.e., $\hat{I}_{\mathrm{s,u}} = \sum_{x \in \bar{\Phi}_{\mathrm{sO}} \setminus s} P_s F_{\mathrm{x,u}} r_{\mathrm{x,u}}^{-\beta}$. Here $\bar{\Phi}_{\mathrm{sO}}$ denotes the PPP of successfully backhauled SBSs in OBFD mode with intensity $\bar{\lambda}_{\mathrm{sO}}$ and can be obtained by using the **mean load approximation** as detailed below in **Remark 3**.

Remark 3 (Intensity of Interfering SBSs in OBFD Mode)**.** Following similar steps as in **Remark 2**, the intensity $\bar{\lambda}_{\mathrm{sO}}$ of the interfering SBSs in OBFD mode can be defined as $(1-q)\min(\lambda_s/\lambda_c, \mathcal{S})\,\lambda_c$.

2) Backhaul link: The received SINR on the backhaul link of an SBS operating in OBFD mode can be modeled as follows:

$$\mathrm{SINR}_{\mathrm{b,O}} = \frac{P_c \; r_{\mathrm{c,s}}^{-\beta}}{I_{\mathrm{s,s}} + I_{\mathrm{c,s}}}, \tag{19}$$

where $I_{\mathrm{s,s}}$ can be given as $I_{\mathrm{s,s}} = \sum_{x \in \bar{\Phi}_{\mathrm{sI}}} P_s \; F_{\mathrm{x,s}} \; r_{\mathrm{x,s}}^{-\beta}$ and $I_{\mathrm{c,s}} = \sum_{y \in \Phi_c \setminus \mathrm{c}} P_c r_{\mathrm{y,s}}^{-\beta}$.

Remark 4 (Backhaul Rate Coverage)**.** Since $\mathcal{N}_s$ is a RV in the desired backhaul link threshold $\gamma_{\mathrm{b,I}}$, the rate coverage of a given SBS in the IBFD mode can be calculated as follows:

$$\mathcal{C}_{\mathrm{I}} = \mathbb{P}(\mathrm{SINR}_{\mathrm{a,I}} > \gamma_{\mathrm{a,I}}) \times \mathbb{E}_{\mathcal{N}_s}\left[\mathbb{P}\left(\frac{P_c \; r_{\mathrm{c,s}}^{-\beta}}{I_{\mathrm{s,s}} + I_{\mathrm{c,s}} + I_{\mathrm{SI}}} > \gamma_{\mathrm{b,I}}\right)\right], \tag{20}$$

where $\mathcal{N}_s \geq 1$. The same method is applicable to the rate coverage of the SBS in OBFD mode.

IV. Downlink Rate Coverage Analysis of IBFD/OBFD SBSs

In this section, we first derive the Laplace transforms of the interferences and then the rate coverage at the backhaul and access links of a generic SBS considering both the IBFD and OBFD modes with Gamma-distributed fading channel powers at the access links. The steps of the analytical approach are:

- Considering the IBFD mode, derive the Laplace transforms of the co-tier and cross-tier interferences received at the user, i.e., $\mathcal{L}_{I_{\mathrm{s,u}}}(t)$ and $\mathcal{L}_{I_{\mathrm{c,u}}}(t)$, respectively.
- Derive the rate coverage at the access link of an SBS in IBFD mode. The rate coverage at the access link in OBFD mode is given as a special case of the IBFD mode.
- Considering the IBFD mode, derive the Laplace transforms of the co-tier and cross-tier interferences received at the SBS, i.e., $\mathcal{L}_{I_{\mathrm{c,s}}}(t)$ and $\mathcal{L}_{I_{\mathrm{s,s}}}(t)$, respectively.
- Derive the rate coverage at the backhaul link of an SBS in IBFD mode. The backhaul rate coverage in OBFD mode is given as a special case of the IBFD mode.
- Finally, the total rate coverage probability of a user in IBFD and OBFD mode, i.e., $\mathcal{C}_I$ and $\mathcal{C}_O$ are obtained using (9) and (10), respectively.

A. Rate Coverage Analysis: Access Links

To derive the rate coverage probability at the access link of a given SBS operating in IBFD mode, we first derive the Laplace transforms of the interferences $I_{\mathrm{s,u}}$ and $I_{\mathrm{c,u}}$ in the following.

Using the definition of the Laplace transform, the Laplace transform of the interference $I_{\mathrm{s,u}}$ can be derived as follows:

$$\mathcal{L}_{I_{\mathrm{s,u}}}(t) = \mathbb{E}_{I_{\mathrm{s,u}}}\left[\exp\left[-tI_{\mathrm{s,u}}\right]\right],$$

$$\overset{(a)}{=} \mathbb{E}_{\bar{\Phi}_{\mathrm{sI}},\{F_{\mathrm{x,u}}\}}\left[\prod_{x\in\bar{\Phi}_{\mathrm{sI}}\setminus \mathrm{s}} \exp\left[-tP_s\, r_{\mathrm{x,u}}^{-\beta}\, F_{\mathrm{x,u}}\right]\right],$$

$$\overset{(b)}{=} \mathbb{E}_{\bar{\Phi}_{\mathrm{sI}}}\left[\prod_{x\in\bar{\Phi}_{\mathrm{sI}}\setminus s} (1+tP_s\, r_{\mathrm{x,u}}^{-\beta}\, \theta_{F_{\mathrm{x,u}}})^{-k_{F_{\mathrm{x,u}}}}\right],$$

$$\overset{(c)}{=} \exp\left[-2\pi\bar{\lambda}_{\mathrm{sI}}\int_{r_{\mathrm{s,u}}}^{\infty}\left(1-\frac{1}{(1+\frac{tP_s\,\theta_{F_{\mathrm{x,u}}}}{r_{\mathrm{x,u}}^{\beta}})^{k_{F_{\mathrm{x,u}}}}}\right) r_{\mathrm{x,u}} dr_{\mathrm{x,u}}\right],$$

$$\overset{(d)}{=} e^{-\pi\bar{\lambda}_{\mathrm{sI}} r_{\mathrm{s,u}}^2\left({}_2F_1\left[k_{F_{\mathrm{x,u}}},-\frac{2}{\beta},1-\frac{2}{\beta},-\frac{tP_s\,\theta_{F_{\mathrm{x,u}}}}{r_{\mathrm{s,u}}^{\beta}}\right]-1\right)}, \tag{21}$$

where (a) follows from the independence of the interfering links, (b) follows from the definition of MGF of a Gamma RV, (c) follows the probability generating functional (PGFL) of PPP, and (d) follows from solving the integral by making substitution $z = (r_{\mathrm{s,u}}/r_{\mathrm{x,u}})^{\beta}$ and performing algebraic manipulations.

Similarly, following (21), the Laplace transform of $I_{\mathrm{c,u}}$ can be expressed as follows:

$$\mathcal{L}_{I_{\mathrm{c,u}}}(t) = \mathbb{E}_{\Phi_{\mathrm{c}}}\left[\prod_{y\in\Phi_{\mathrm{c}}} \exp\left[-tP_c r_{\mathrm{y,u}}^{-\beta}\right]\right],$$

$$\overset{(a)}{=} \exp\left[-2\pi\lambda_c\int_0^{\infty}\left(1-\exp\left[-tP_c r_{\mathrm{y,u}}^{-\beta}\right]\right) r_{\mathrm{y,u}}\mathrm{d}r_{\mathrm{y,u}}\right],$$

$$\overset{(b)}{=} \exp\left[-\pi\lambda_c (tP_c)^{\frac{2}{\beta}}\Gamma\left(1-\frac{2}{\beta}\right)\right], \tag{22}$$

where (a) follows from the PGFL of a PPP and (b) follows from solving the integral in (a). Note that the integral in (22) has a lower limit of zero as the nearest CN of a user can be arbitrarily close to the user.

The rate coverage at the access link of an SBS in IBFD mode can then be formulated as follows.

Lemma 1 (Access Link Rate Coverage of an SBS in IBFD Mode: Gamma Fading Channels)**.** *The coverage probability at the access link of an IBFD SBS can be derived in Gamma fading channels as*

$$\mathbb{P}(\mathrm{SINR}_{\mathrm{a,I}} > \gamma_{\mathrm{a,I}}) = \mathbb{P}\left(\frac{P_s\, F_{\mathrm{s,u}}\, r_{\mathrm{s,u}}^{-\beta}}{\underbrace{I_{\mathrm{s,u}}+I_{\mathrm{c,u}}}_{I_{\mathrm{agg}}}+N_0} > \gamma_{\mathrm{a,I}}\right),$$

$$= 2\pi\lambda_s\int_0^{\infty} F_{I_{\mathrm{agg}}}\left(\frac{P_s\, F_{\mathrm{s,u}}}{\gamma_{\mathrm{a,I}} r_{\mathrm{s,u}}^{\beta}} - N_0\right) r_{\mathrm{s,u}} e^{-\pi\lambda_s {r_{\mathrm{s,u}}}^2} dr_{\mathrm{s,u}}. \tag{23}$$

Since fading in the desired channel follows a Gamma distribution, we resort to apply the Gil-Pelaez inversion theorem to evaluate the rate coverage probability. The CDF of the aggregate interference $F_{I_{\mathrm{agg}}}(\cdot)$ can be derived as detailed below:

$$F_{I_{\mathrm{agg}}}\left(\frac{P_s\, F_{\mathrm{s,u}}}{r_{\mathrm{s,u}}^{\beta}\gamma_{\mathrm{a,I}}} - N_0\right)$$

$$\overset{(a)}{=} \frac{1}{2} - \frac{1}{\pi}\int_0^{\infty} \mathrm{Im}\left[\mathcal{L}_{I_{\mathrm{agg}}}(-jw)\, e^{-jw\left(\frac{P_s\, F_{\mathrm{s,u}}}{r_{\mathrm{s,u}}^{\beta}\gamma_{\mathrm{a,I}}}-N_0\right)}\right]\frac{dw}{w},$$

$$\overset{(b)}{=} \frac{1}{2} - \frac{1}{\pi}\int_0^{\infty} \mathrm{Im}\left[\mathcal{L}_{I_{\mathrm{c,u}}}(-jw)\,\mathcal{L}_{I_{\mathrm{s,u}}}(-jw) \times \mathcal{L}_{F_{\mathrm{s,u}}}\left(j\frac{P_s w}{r_{\mathrm{s,u}}^{\beta}\gamma_{\mathrm{a,I}}}\right) e^{jwN_0}\right]\frac{dw}{w}, \tag{24}$$

where $\mathrm{Im}(\cdot)$ represents the imaginary part of the argument. Using (23), (a) follows from the application of the Gil-Pelaez inversion theorem and (b) follows from the independence of $I_{\mathrm{s,u}}$ and $I_{\mathrm{c,u}}$ and applying the definition of the Laplace transform of $F_{\mathrm{s,u}}$ where $\mathcal{L}_{F_{\mathrm{s,u}}}(jw)$ can be given as follows:

$$\mathcal{L}_{F_{\mathrm{s,u}}}\left(j\frac{P_s w}{r_{\mathrm{s,u}}^{\beta}\gamma_{\mathrm{a,I}}}\right) = \left(1+j\frac{P_s w}{r_{\mathrm{s,u}}^{\beta}\gamma_{\mathrm{a,I}}}\theta_{F_{\mathrm{s,u}}}\right)^{-k_{F_{\mathrm{s,u}}}}. \tag{25}$$

Remark 5 (Access Link Rate Coverage of an SBS in OBFD Mode)**.** Similar to the IBFD mode in (21), the Laplace transform of $\hat{I}_{\mathrm{s,u}}$ can be obtained as $\mathcal{L}_{\hat{I}_{\mathrm{s,u}}}(t) = \mathbb{E}_{\bar{\Phi}_{\mathrm{sO}}}\left[\prod_{x\in\bar{\Phi}_{\mathrm{sO}}\setminus s}(1+tP_s\, r_{\mathrm{x,u}}^{-\beta}\,\theta_{F_{\mathrm{x,u}}})^{-k_{F_{\mathrm{x,u}}}}\right]$. A closed-form expression can be given by replacing $\bar{\lambda}_{\mathrm{sI}}$ in (21) with $\bar{\lambda}_{\mathrm{sO}}$. Consequently, the rate coverage at the access link of an SBS in OBFD mode can be derived by replacing $\gamma_{\mathrm{a,I}}$ with $\gamma_{\mathrm{a,O}}$ and $F_{I_{\mathrm{agg}}}$ with $F_{\hat{I}_{\mathrm{s,u}}}$ in **Lemma 1** mentioned above.

B. Rate Coverage Analysis: Backhaul Links

Now we derive the Laplace transforms of the interferences in the backhaul link of a given SBS operating in IBFD mode, i.e., $I_{\mathrm{s,s}}$ and $I_{\mathrm{c,s}}$. The Laplace transform of $I_{s,s}$ can be obtained as $\mathcal{L}_{I_{\mathrm{s,s}}}(t) = \mathbb{E}_{\bar{\Phi}_{\mathrm{sI}}}\left[\prod_{x\in\bar{\Phi}_{\mathrm{sI}}}(1+tP_s\, r_{\mathrm{x,s}}^{-\beta}\,\theta_{F_{\mathrm{x,s}}})^{-k_{F_{\mathrm{x,s}}}}\right]$. A closed-form expression can then be given simplifying the result in Eq. (21)(d) for $r_{\mathrm{s,u}} \to 0$ as follows:

$$\mathcal{L}_{I_{\mathrm{s,s}}}(t) = \lim_{r_{\mathrm{s,u}}\to 0} e^{-\pi\bar{\lambda}_{\mathrm{sI}} r_{\mathrm{s,u}}^2\,{}_2F_1\left[k_{F_{\mathrm{x,u}}},-\frac{2}{\beta},1-\frac{2}{\beta},-\frac{tP_s\,\theta_{F_{\mathrm{x,u}}}}{r_{\mathrm{s,u}}^{\beta}}\right]},$$

$$\overset{(a)}{=} \lim_{r_{\mathrm{s,u}}\to 0} e^{-\pi\bar{\lambda}_{\mathrm{sI}}\frac{{}_2F_1\left[1-\frac{2}{\beta}-k_{F_{\mathrm{x,u}}},-\frac{2}{\beta},1-\frac{2}{\beta},\frac{tP_s\,\theta_{F_{\mathrm{x,u}}}}{r_{\mathrm{s,u}}^{\beta}+tP_s\,\theta_{F_{\mathrm{x,u}}}}\right]}{\left(r_{\mathrm{s,u}}^{\beta}+tP_s\,\theta_{F_{\mathrm{x,u}}}\right)^{-\frac{2}{\beta}}}},$$

$$= \exp\left[-\pi\bar{\lambda}_{\mathrm{sI}}\frac{{}_2F_1\left[1-\frac{2}{\beta}-k_{F_{\mathrm{x,u}}},-\frac{2}{\beta},1-\frac{2}{\beta},1\right]}{\left(tP_s\,\theta_{F_{\mathrm{x,u}}}\right)^{-\frac{2}{\beta}}}\right],$$

$$\overset{(b)}{=} \exp\left[-\pi\bar{\lambda}_{\mathrm{sI}}\left(\frac{2\mathcal{B}\left[k_{F_{\mathrm{x,s}}}+\frac{2}{\beta},-\frac{2}{\beta}\right]}{\beta(tP_s\,\theta_{F_{\mathrm{x,s}}})^{-\frac{2}{\beta}}}\right)\right], \tag{26}$$

where (a) follows from Pfaff identity, i.e.,

$${}_2F_1(a,b,c,z) = (1-z)^{-b}\,{}_2F_1\left[c-a,b,c,\frac{z}{z-1}\right],$$

and (b) follows from the definition of Gauss's Hypergeometric function, i.e.,

$${}_2F_1(a,b,c,z) = \frac{\Gamma(c)\Gamma(c-a-b)}{\Gamma(c-a)\Gamma(c-b)},$$

and applying the definition of Beta function.

The Laplace transform of $I_{\mathrm{c,s}}$ can be derived by following the steps in (22) as follows:

$$\mathcal{L}_{I_{\mathrm{c,s}}}(t) = \exp\left[-2\pi\lambda_c \int_{r_{\mathrm{c,s}}}^{\infty} \left(1-\exp\left[-tP_c r_{\mathrm{y,s}}^{-\beta}\right]\right) r_{\mathrm{y,s}} \mathrm{d}r_{\mathrm{y,s}}\right],$$
$$= \exp\left[-\pi\lambda_c \left(\frac{\Gamma\left(1-\frac{2}{\beta}\right)+\frac{2}{\beta}\Gamma_u\left(-\frac{2}{\beta},\frac{tP_c}{r_{\mathrm{c,s}}^{\beta}}\right)}{(tP_c)^{-\frac{2}{\beta}}} - r_{\mathrm{c,s}}^2\right)\right]. \quad (27)$$

We apply Gil-Pelaez inversion theorem to evaluate the rate coverage probability for an SBS in the backhaul link as shown below.

Lemma 2 (Backhaul Link Rate Coverage of an SBS in IBFD Mode)**.** *With Gamma-distributed interfering links, the coverage probability of the backhaul link of an SBS in IBFD mode can be derived as follows:*

$$\mathbb{P}(\mathrm{SIR}_{\mathrm{b,I}} > \gamma_{\mathrm{b,I}})$$
$$= 2\pi\lambda_c \int_0^{\infty} F_{I_{\mathrm{agg}}}\left(\frac{P_c}{\gamma_{\mathrm{b,I}} r_{\mathrm{c,s}}^{\beta}} - I_{\mathrm{SI}}\right) r_{\mathrm{c,s}} e^{-\pi\lambda_c {r_{\mathrm{c,s}}}^2} dr_{\mathrm{c,s}},$$

where $F_{I_{\mathrm{agg}}}(\cdot)$ can be derived as

$$F_{I_{\mathrm{agg}}}\left(\frac{P_c}{\gamma_{\mathrm{b,I}} r_{\mathrm{c,s}}^{\beta}} - I_{\mathrm{SI}}\right)$$
$$= \frac{1}{2} - \frac{1}{\pi}\int_0^{\infty} \mathrm{Im}\left[\frac{\mathcal{L}_{I_{\mathrm{c,s}}}(-jw)\,\mathcal{L}_{I_{\mathrm{s,s}}}(-jw)}{e^{jw\left(\frac{P_c}{\gamma_{\mathrm{b,I}} r_{\mathrm{c,s}}^{\beta}} - I_{\mathrm{SI}}\right)}}\right]\frac{dw}{w}. \quad (28)$$

Remark 6 (Backhaul Link Rate Coverage for an SBS in OBFD Mode)**.** Similar to the IBFD mode, the Laplace transform of $I_{\mathrm{s,s}}$ and $I_{\mathrm{c,s}}$ in OBFD mode can be given as in (26) and (27), respectively. The received SIR at the backhaul link of an SBS operating in OBFD mode (i.e., $\mathrm{SIR}_{\mathrm{b,O}}$) is thus similar to that of an SBS operating in the IBFD mode in (16). Hence, (28) can be used for the OBFD case after replacing $\gamma_{\mathrm{b,I}}$ with $\gamma_{\mathrm{b,O}}$ and substituting $I_{\mathrm{SI}} = 0$.

V. Simplified Rate Coverage Expressions: Specific Scenarios and Approximations

In this section, we provide simplified expressions for an interference-limited scenario with Rayleigh fading at the access links. Moreover, we exploit an approximation of the Gauss's hypergeometric function to further simplify the rate coverage expressions in the access link. Based on the simplified expressions and considering ideal backhaul rate coverage, we derive closed-form expressions for (i) the value of q that maximizes the rate coverage probability of a typical user; (ii) the value of q at which the the rate coverage probability of all SBSs operating in IBFD and OBFD mode in a small cell network can be balanced.

A. Simplified Rate Coverage for Rayleigh Fading

The simplified rate coverage probability expressions in the access link of an IBFD SBS can be derived in closed-form for a typical Rayleigh fading interference-limited scenario as described in the following.

Lemma 3 (Access Link Rate Coverage for an SBS in IBFD Mode in Rayleigh Fading Channels)**.** *For Rayleigh fading channels, i.e., $F_{\mathrm{s,u}} \sim \mathrm{Gamma}(1, \theta_{F_{\mathrm{s,u}}})$ and interference-limited regime, the rate coverage probability experienced at the access link of an IBFD SBS can be simplified as follows:*

$$\mathbb{P}(\mathrm{SIR}_{\mathrm{a,I}} > \gamma_{\mathrm{a,I}}) \overset{(a)}{=} \mathbb{E}\left[\exp\left(-\frac{\gamma_{\mathrm{a,I}} r_{\mathrm{s,u}}^{\beta}}{P_s \theta_{F_{\mathrm{s,u}}}}(I_{\mathrm{c,u}} + I_{\mathrm{s,u}})\right)\right],$$
$$\overset{(b)}{=} \int_0^{\infty} \mathcal{L}_{I_{\mathrm{s,u}}}\left(\frac{\gamma_{\mathrm{a,I}} r_{\mathrm{s,u}}^{\beta}}{P_s \theta_{F_{\mathrm{s,u}}}}\right) \mathcal{L}_{I_{\mathrm{c,u}}}\left(\frac{\gamma_{\mathrm{a,I}} r_{\mathrm{s,u}}^{\beta}}{P_s \theta_{F_{\mathrm{s,u}}}}\right) f_{r_{\mathrm{s,u}}}(r_{\mathrm{s,u}}) dr_{\mathrm{s,u}},$$
$$\overset{(c)}{=} \frac{\lambda_s}{\bar{\lambda}_{\mathrm{SI}}\left({}_2F_1\left[1, -\frac{2}{\beta}, 1-\frac{2}{\beta}, -\gamma_{\mathrm{a,I}}\right] - 1\right) + \lambda_s + A}, \quad (29)$$

where $A = \Gamma\left(1-\frac{2}{\beta}\right)\lambda_c\left(\frac{\gamma_{\mathrm{a,I}} P_c}{P_s \theta_{F_{\mathrm{s,u}}}}\right)^{\frac{2}{\beta}}$ and is independent of q.

Note that (a) follows from the CDF of the exponential distribution with average power $\theta_{F_{\mathrm{s,u}}}$, (b) follows from the definition of Laplace transform and the independence of $I_{\mathrm{c,u}}$ and $I_{\mathrm{s,u}}$, and (c) follows from substituting (21) and (22) and evaluating the integral.

The backhaul rate coverage expressions can also be simplified for Rayleigh fading channels due to the simplification of Beta function in $\mathcal{L}_{I_{\mathrm{s,s}}}(t)$ as follows:

$$\mathcal{L}_{I_{\mathrm{s,s}}}(t) = \exp\left[-\frac{2\pi^2 \bar{\lambda}_{\mathrm{SI}} \mathrm{csc}(\frac{2\pi}{\beta})}{(tP_s\,\theta_{F_{\mathrm{x,s}}})^{-\frac{2}{\beta}}\beta}\right]. \quad (30)$$

B. Approximate Rate Coverage for Gamma/Rayleigh Fading

From [24, 13, Ch. 5, Eq. (2)], we have ${}_2F_1\left[-\frac{2}{\beta}, k, 1-\frac{2}{\beta}, jx\right] \approx 1 - \frac{j2xk}{\beta-2}$. With this approximation, the rate coverage expressions in the access link can be further simplified for both Gamma and Rayleigh fading channels. The Rayleigh fading case is detailed below.

Corollary 1 (Approximate Access Link Rate Coverage for an SBS in IBFD/OBFD Mode Under Rayleigh Fading Channels)**.** *With the aforementioned approximation, the rate coverage probability experienced at the access link of an SBS in IBFD mode can be simplified as follows:*

$$\mathbb{P}(\mathrm{SIR}_{\mathrm{a,I}} > \gamma_{\mathrm{a,I}}) \approx \frac{\lambda_s}{\bar{\lambda}_{\mathrm{SI}}\frac{2}{\beta-2}\gamma_{\mathrm{a,I}} + \lambda_s + \Gamma\left(1-\frac{2}{\beta}\right)\lambda_c\left(\frac{\gamma_{\mathrm{a,I}} P_c}{P_s \theta_{F_{\mathrm{s,u}}}}\right)^{\frac{2}{\beta}}}. \quad (31)$$

Similarly, the approximate access link rate coverage expression for OBFD mode can be derived as follows:

$$\mathbb{P}(\mathrm{SIR}_{\mathrm{a,O}} > \gamma_{\mathrm{a,O}}) \approx \frac{\lambda_s}{\bar{\lambda}_{\mathrm{SO}}\frac{2}{\beta-2}\gamma_{\mathrm{a,O}} + \lambda_s}. \quad (32)$$

In the interference-limited regime and perfect backhaul coverage, it can be observed that the rate coverage in the access link of an SBS in IBFD mode is vulnerable to both the transmit powers and intensities of CNs and SBSs. On the other hand, the rate coverage of an SBS in OBFD mode is independent

of the transmit powers of CNs or SBSs. Furthermore, if the average load per CN is less than $\mathcal{S}$, the rate coverage of an SBS in OBFD mode becomes independent of the intensities of CNs or SBSs. This can be verified by substituting the value of $\bar{\lambda}_{\mathrm{SO}}$ in **Corollary 1**. These observations become more evident when $M \to \infty$ and in turn $\gamma_{\mathrm{b,I}}, \gamma_{\mathrm{b,O}} \to 0$.

C. Perfect Backhaul Coverage: Large Values of M

The ideal backhaul rate coverage can be realized when the ratio $\frac{M}{\min(\mathcal{N}_s,\mathcal{S})}$ becomes very large, i.e., $\gamma_{\mathrm{b,I}}$ and $\gamma_{\mathrm{b,O}}$ become very small as can be observed from (8). In such a case, we can customize the value of q in closed-form such that either the user's rate coverage is maximized (i.e., q^*) or the rate coverage of all SBSs in the network (in IBFD or OBFD mode) becomes balanced (i.e., q^{balance}).

The optimization of rate coverage leads to optimized network performance when each SBS can adaptively serve its associated user in both the IBFD and OBFD modes. That is, each SBS can set the optimal proportion q^* to switch between IBFD and OBFD modes. Nonetheless, all SBSs may not have the capability to adaptively switch into different modes or some BSs can only operate in OBFD mode (could be due to unavailability of advanced SI cancellation circuitry or any other implementation issues). In such a case, a user connected to an IBFD SBS will experience significantly different rate coverage probability from a user connected to an OBFD SBS depending on the proportion of IBFD and OBFD SBSs in the network. Consequently, it will be important to set the proportion of IBFD SBSs in the network such that they do not hurt the rate coverage probability of users associated to OBFD SBSs. The proportion which balances the rate coverage in all IBFD and OBFD SBSs q^{balance} can be decided in advance so that each user can experience the same rate coverage.

In the following, we derive both the q^* and q^{balance} in closed-form.

Corollary 2 (Balanced Rate Coverage with Perfect Backhaul Rate Coverage)**.** *In order to balance the rate coverage among all IBFD and OBFD SBSs in the network, we equate* $\mathbb{P}(\mathrm{SIR}_{\mathrm{a,O}} > \gamma_{\mathrm{a,O}})$ *and* $\mathbb{P}(\mathrm{SIR}_{\mathrm{a,I}} > \gamma_{\mathrm{a,I}})$ *that leads to* $\bar{\lambda}_{\mathrm{SO}}\ {}_2F_1\left[1,-\frac{2}{\beta},1-\frac{2}{\beta},-\gamma_{\mathrm{a,O}}\right] - \bar{\lambda}_{\mathrm{SI}}\ {}_2F_1\left[1,-\frac{2}{\beta},1-\frac{2}{\beta},-\gamma_{\mathrm{a,I}}\right] = A + \bar{\lambda}_{\mathrm{SO}} - \bar{\lambda}_{\mathrm{SI}}$. *Substituting the expressions of* $\bar{\lambda}_{\mathrm{SI}}$ *and* $\bar{\lambda}_{\mathrm{SO}}$ *from* **Remark 2** *and* **Remark 3** *we can derive* q *as follows:*

$$q^{\mathrm{balance}} = \frac{{}_2F_1\left[1,-\frac{2}{\beta},1-\frac{2}{\beta},-\gamma_{\mathrm{a,O}}\right]-1-\frac{A}{\lambda_c\min(\lambda_s/\lambda_c,\mathcal{S})}}{{}_2F_1\left[1,-\frac{2}{\beta},1-\frac{2}{\beta},-\gamma_{\mathrm{a,O}}\right]+{}_2F_1\left[1,-\frac{2}{\beta},1-\frac{2}{\beta},-\gamma_{\mathrm{a,I}}\right]-2}. \tag{33}$$

Also, in this case, the access link rate coverage of a typical user defined as $\mathcal{C}_u = q\mathbb{P}(\mathrm{SIR}_{\mathrm{a,I}} > \gamma_{\mathrm{a,I}}) + (1-q)\mathbb{P}(\mathrm{SIR}_{\mathrm{a,O}} > \gamma_{\mathrm{a,O}})$ can be optimized with respect to q. However, the presence of ${}_2F_1(\cdot)$ in the expression makes it difficult to obtain direct insights. As such, we approximate ${}_2F_1(\cdot)$ as in **Corollary 1**. In the following, we derive a more simplified closed-form expression of q^{balance}.

Corollary 3 (Approximate Balanced Rate Coverage with Perfect Backhaul Rate Coverage)**.** *In order to balance the rate coverage in IBFD as well as OBFD mode, we equate* $\mathbb{P}(\mathrm{SIR}_{\mathrm{a,O}} > \gamma_{\mathrm{a,O}})$ *and* $\mathbb{P}(\mathrm{SIR}_{\mathrm{a,I}} > \gamma_{\mathrm{a,I}})$. *Substituting the expressions of* $\bar{\lambda}_{\mathrm{SI}}$ *and* $\bar{\lambda}_{\mathrm{SO}}$ *from* **Remark 2** *and* **Remark 3** *we can derive* q *as follows:*

$$q^{\mathrm{balance}} = \frac{\gamma_{\mathrm{a,O}} - \frac{A(\beta-2)}{2\lambda_c\min(\lambda_s/\lambda_c,\mathcal{S})}}{\gamma_{\mathrm{a,I}} + \gamma_{\mathrm{a,O}}}. \tag{34}$$

Note that q^{balance} is inversely proportional to A and in turn the transmission powers of CNs and SBSs, i.e., $\frac{P_c}{P_s}$. Moreover, when the average load per CN is less than the $\mathcal{S}$, q^{balance} becomes inversely proportional to the factor $\frac{\lambda_s}{\lambda_c}$. That is, increasing the intensity/power of SBSs requires an increase in the fraction of SBSs operating in IBFD mode to maintain a fair rate coverage at all SBSs in a small cell network.

Similarly, the rate coverage of a typical user in the access link can be optimized with respect to q as detailed below.

Corollary 4 (Optimal Rate Coverage of a Typical User with Perfect Backhaul Rate Coverage)**.** *Assuming perfect backhaul coverage, using the relation* $\mathcal{C}_u = q\mathcal{C}_{\mathrm{I}} + (1-q)\mathcal{C}_{\mathrm{O}}$ *for rate coverage and substituting* $\mathcal{C}_{\mathrm{I}}$ *and* $\mathcal{C}_{\mathrm{O}}$ *from eq. (31) and eq. (32) yields*

$$\mathcal{C}_u = \frac{q\lambda_s}{\bar{\lambda}_{\mathrm{SI}}\frac{2}{\beta-2}\gamma_{\mathrm{a,I}} + \lambda_s + A} + \frac{(1-q)\lambda_s}{\bar{\lambda}_{\mathrm{SO}}\frac{2}{\beta-2}\gamma_{\mathrm{a,O}} + \lambda_s} \tag{35}$$

Since $\bar{\lambda}_{\mathrm{SI}} = q \times \min(\lambda_s/\lambda_c,\mathcal{S})\lambda_c$ *and* $\bar{\lambda}_{\mathrm{SO}} = (1-q) \times \min(\lambda_s/\lambda_c,\mathcal{S})\lambda_c$, *we can write*

$$\mathcal{C}_u = \frac{q\lambda_s}{qc\gamma_{\mathrm{a,I}} + \lambda_s + A} + \frac{(1-q)\lambda_s}{(1-q)c\gamma_{\mathrm{a,O}} + \lambda_s}, \tag{36}$$

where $c = \frac{2\lambda_c \times \min(\lambda_s/\lambda_c,\mathcal{S})}{\beta-2}$. *Now differentiating each term with respect to* q *yields*

$$\frac{d\mathcal{C}_u}{dq} = \lambda_s\left(\frac{A+\lambda_s}{(A+cq\gamma_{\mathrm{a,I}}+\lambda_s)^2} - \frac{\lambda_s}{(c\gamma_{\mathrm{a,O}}(1-q)+\lambda_s)^2}\right). \tag{37}$$

An optimum q *for a typical user can then be given as follows:*

$$q^* = \frac{(A+\lambda_s)(c^2\gamma_{\mathrm{a,O}}^2+d) \pm (c(A+c\gamma_{\mathrm{a,I}})\gamma_{\mathrm{a,O}}+d)\sqrt{\lambda_s(A+\lambda_s)}}{c^2(-\gamma_{\mathrm{a,I}}^2\lambda_s+\gamma_{\mathrm{a,O}}^2(A+\lambda_s))}, \tag{38}$$

where $d = c(\gamma_{\mathrm{a,I}}+\gamma_{\mathrm{a,O}})\lambda_s$. *Note that* $(A+\lambda_s)(c^2\gamma_{\mathrm{a,O}}^2+d) > c^2(-\gamma_{\mathrm{a,I}}^2\lambda_s+\gamma_{\mathrm{a,O}}^2(A+\lambda_s))$ *and* $0 \le q \le 1$, *thus the root with a negative sign is feasible only.*

By replacing $c = \lambda_c \times \min(\lambda_s/\lambda_c,\mathcal{S})$, $\gamma_{\mathrm{a,I}} = {}_2F_1[1,-\frac{2}{\beta},1-\frac{2}{\beta},-\gamma_{\mathrm{a,I}}] - 1$, and $\gamma_{\mathrm{a,O}} = {}_2F_1[1,-\frac{2}{\beta},1-\frac{2}{\beta},-\gamma_{\mathrm{a,O}}] - 1$, (38) can be used to obtain q^* without approximation.

VI. Backhaul Interference Mitigation Techniques

Since the backhaul interference incurred at a user terminal appears to be a fundamental bottleneck in the performance of in-band wireless backhauling, some kind of coordination between CNs and SBSs is crucial to achieve the performance gains of IBFD over OBFD mode. In this context, this section first discusses a distributed backhaul aware mode selection mechanism which provides some further insights into selecting the proportion of in-band and out-of-band SBSs (q) as a function of network parameters. We then discuss two solution

techniques that can potentially enhance the performance of in-band wireless backhauling, namely, Backhaul Interference-Aware (BIA) power control at CNs and Interference Rejection (IR) from the CN the serving SBS of the typical user is associated with. Since the locations of the BSs are relatively fixed, the aforementioned backhaul interference management techniques can be easily implemented in practice.

A. Distributed Backhaul-Aware IBFD/OBFD Mode Selection

Based on the received power at a certain user from both the nearest CN and its serving SBS, the serving SBS independently chooses its mode, i.e., IBFD or OBFD mode. In practice, this mode selection can also be performed by the user as the interference estimation could be much easier at the user's end in the downlink. The user can then inform its designated SBS about the feasible mode of operation.

Specifically, the SBS chooses the IBFD mode if the received signal power from that SBS at the user is sufficiently higher than the power received from the strongest interfering CN. In such a case, using more radio resources by switching to the OBFD mode is not necessary. On the other hand, if the signal power at the user from the strongest interfering CN is comparable or higher than the useful signal power received from its serving SBS, the OBFD mode of operation is selected. The mode selection criterion can be written mathematically as:

$$\begin{cases} \frac{P_s r_{\mathrm{s0,u}}^{-\beta}}{P_c r_{\mathrm{c0,u}}^{-\beta}} \geq \tau, & \text{IBFD mode} \\ \frac{P_s r_{\mathrm{s0,u}}^{-\beta}}{P_c r_{\mathrm{c0,u}}^{-\beta}} < \tau, & \text{OBFD mode} \end{cases} \tag{39}$$

where τ is a threshold that can be different for each user and can be chosen as a function of the target rate requirement of that user, $r_{\mathrm{s0,u}}$ is the distance from the user to its serving SBS and $r_{\mathrm{c0,u}}$ is the distance from the same user to its closest CN. Given the mode selection criterion, the expression for q can be derived for path-loss only environment as follows:

$$\begin{aligned} q &= \mathbb{E}_{r_{\mathrm{s0,u}}}\left[\mathbb{P}\left[r_{\mathrm{c0,u}} > \left(\frac{\tau P_c}{P_s}\right)^{\frac{1}{\beta}} r_{\mathrm{s0,u}}\right]\right], \\ &\overset{(a)}{=} \int_0^\infty \exp\left[-\pi\lambda_c \left(\frac{\tau P_c}{P_s}\right)^{\frac{2}{\beta}} r^2\right] \cdot 2\pi\lambda_s r \exp\left[-\pi\lambda_s r^2\right] \mathrm{d}r, \\ &= \left(1 + \frac{\lambda_c}{\lambda_s}\left(\tau\frac{P_c}{P_s}\right)^{\frac{2}{\beta}}\right)^{-1}, \end{aligned} \tag{40}$$

where (a) follows by using the distribution of distance to the nearest point in a PPP. Note that, τ is a design parameter which plays a key role in controlling the trade-off between the rate coverage and the backhaul interference. Intuitively, in case when the backhaul interference from the nearest CN is more dominant, τ can be comparable to $\gamma_{\mathrm{a,I}}$ or $\gamma_{\mathrm{a,O}}$. However, in the other case τ should be selected sufficiently higher than $\gamma_{\mathrm{a,I}}$ or $\gamma_{\mathrm{a,O}}$ to consider the impact of additional co-tier and cross-tier interferences.

As has been mentioned in previous sections, for a given set of network parameters, a network designer can determine the optimized value of q given the statistical knowledge/distributions of the intensity and locations of the CNs, SBSs, users, and channel gains among them. The optimal value of q can then be broadcast to all SBSs in the system. However, a given SBS can also decide the mode in a distributed manner (e.g., by using (40)). Nonetheless, since the decisions of a SBS are dependent only on the statistics of its users' channels and the incurred backhaul interference, the distributed mode selection can lead to performance degradation (especially if the threshold τ is not optimized). This will be demonstrated via numerical results in Section VII.

B. Interference Rejection

For massive MIMO systems, backhaul interference at a given user from the CN its SBS is associated with can be completely rejected. This can be done by designing precoders assuming full knowledge of the channel state information (CSI) between that CN and all users within its coverage [16]. For example, if $\mathbf{H}_{\mathrm{c,u}}$ is the $1 \times M$ channel vector between the CN and a given user u, the interference at u from that CN can be canceled (or rejected) by multiplying the transmit signal (i.e., beamforming) from the CN by the matrix $\mathbf{R}(\mathbf{H}_{\mathrm{c,s}} \cdot \mathbf{R})^\dagger$ where $\mathbf{H}_{\mathrm{c,s}}$ is the channel vector between the serving SBS of u and its serving CN, $(\cdot)^\dagger$ denotes the pseudo inverse, and $\mathbf{R}$ is calculated to satisfy the condition $\mathbf{H}_{\mathrm{c,u}} \cdot \mathbf{R} = \mathbf{0}$. In this case, the channel gain between this CN and the user served by its associated SBS is $\mathbf{H}_{\mathrm{c,u}}\mathbf{R}(\mathbf{H}_{\mathrm{c,s}} \cdot \mathbf{R})^\dagger = \mathbf{0}(\mathbf{H}_{\mathrm{c,s}} \cdot \mathbf{R})^\dagger = \mathbf{0}$. Note that, the number of antenna M needs to be greater than or equal to $2 \times \min(\mathcal{N}_s, \mathcal{S})$ (i.e., the total number of SBS and the associated users under the assumption that one user is served per SBS at a time).

As such, the interference in (15) reduces to the following:

$$I_{\mathrm{c,u}} = \sum_{y \in \Phi_c} P_c r_{\mathrm{y,u}}^{-\beta} = \sum_{y \in \Phi_c \setminus c} P_c \, r_{\mathrm{y,u}}^{-\beta}. \tag{41}$$

Hence, using (27), the Laplace transform of the backhaul interference can be given as follows:

$$\mathcal{L}_{I_{\mathrm{c,u}}}(t) = \mathcal{L}_{I_{\mathrm{c,s}}}(t)\,|_{r_{\mathrm{c,s}} = r_{\mathrm{c,u}}}. \tag{42}$$

C. Backhaul Interference-Aware (BIA) Power Control at CNs

BIA power control scheme requires the following information at a given CN c, i.e.,

- the cumulative interference at a given IBFD SBS s associated with that CN c ($I_{\mathrm{agg}} = I_{\mathrm{c,s}} + I_{\mathrm{s,s}} + I_{\mathrm{SI}}$),
- the desired link between CN c and the IBFD SBS s, and
- the desired target SIR of the backhaul link $\gamma_{\mathrm{b,I}}$.

Based on these informations, a given CN reduces its power to a given IBFD SBS from $\frac{P_c}{\min(\mathcal{N}_s, \mathcal{S})}$ to a level that can strictly ensure $\gamma_{\mathrm{b,I}}$. Otherwise, the CN continues to transmit with power $\frac{P_c}{\min(\mathcal{N}_s, \mathcal{S})}$. This power reduction can potentially reduce the cross-tier interference experienced at a user associated with IBFD SBS s. Mathematically, the power level of a CN can then be defined as follows:

$$P_{\mathrm{cn}}^s = \min\left(\frac{P_c}{\min(\mathcal{N}_s, \mathcal{S})}, \frac{\gamma_{\mathrm{b,I}} I_{\mathrm{agg}}}{r_{\mathrm{c,s}}^{-\beta} S_{\mathrm{c,s}}}\right). \tag{43}$$

However, since the factor $\min(\mathcal{N}_s, \mathcal{S})$ is already considered in the definition of $\gamma_{\mathrm{b,I}}$ (see (2) and (8)), thus we can write:

$$P_{\mathrm{cn}}^{s} = \min\left(P_c, \frac{\gamma_{\mathrm{b,I}} I_{\mathrm{agg}}}{r_{\mathrm{c,s}}^{-\beta} S_{\mathrm{c,s}}}\right). \tag{44}$$

In practice, the aforementioned CSI is most likely available at all SBSs and thus the calculation of the desired power from CN, i.e., $\frac{\gamma_{\mathrm{b,I}} I_{\mathrm{agg}}}{r_{\mathrm{c,s}}^{-\beta} S_{\mathrm{c,s}}}$ can be performed by SBS and then forwarded to CN. Based on the load of associated SBSs per CN, the CN can decide the transmit power level. Note that the gains of BIA power control scheme are expected to be more evident in the following scenarios:

- reduced number of SBSs per CN,
- low values of $\gamma_{\mathrm{b,I}}$, and
- high total transmit power P_c of a given CN.

In the above scenarios, equal transmit power allocation per backhaul stream at CN results in unnecessarily high transmission power. As such, the significance of applying the adaptive power control at a CN per IBFD stream is evident.

VII. Numerical and Simulation Results

In this section, we validate the accuracy of the derived expressions. The downlink coverage probability of a typical user and an SBS in both IBFD and OBFD modes is investigated in terms of the density of SBSs, the SI value of the IBFD SBSs, and the transmit power of the CN. Performance trade-offs are characterized and insights are extracted related to the feasibility and selection of in-band or out-of-band backhaul modes for FD small cells.

For our simulation results, we consider the path-loss exponent $\beta = 4$ and the intensity of CNs as $\lambda_c' = 10$. Note that the simulations consider the shadowing phenomenon explicitly. As such, the used intensities for CNs and SBSs are the intensities (i.e., λ_c' and λ_s') defined prior to using the displacement theorem in **Remark 1**. The total transmit power available at each CN and SBS is taken as P_c = 10W and P_s = 2W, respectively. The number of available antennas at each CN is $M = 500$ and the number of supported backhaul streams per CN is $S = 50$. The required rate on a given transmission channel is set as $R_{\mathrm{th}} = 1$ bps/Hz. The SI cancellation value ξ is set to 120 dB. Log-Normal shadowing channel for the desired and interfering access links are modeled with parameters $\mu = 1$ and $\sigma = 2$. The Gamma-distributed fading channel powers experienced at the SBS and at the user are modeled with shape parameters $k = 0.5$ and $k = 2$, respectively, with the average channel fading power $k\theta = 1$. The values of the above-mentioned parameters remain the same unless stated otherwise.

In the Monte-Carlo simulations, the SBSs, CNs, and users are generated randomly in a circular cellular region in each iteration. Their numbers follow a Poisson distribution while their locations are randomly distributed in the cellular region following a uniform distribution. In each iteration, based on the randomly generated channel gains (composed of distance-based path-loss, shadowing, and fading) of access and backhaul links, different kind of interferences and in turn the attained SINR at the access and backhaul links is calculated. Since we assume perfect channel estimation and zero-forcing beamforming, the impact of pilot-contamination and intra-cell interference is ignored in the simulations. Moreover, in case of interference rejection, we ignore the backhaul interference from the CN the SBS of a typical user is associated with.

A. Rate Coverage vs. Fraction of SBSs in IBFD/OBFD Mode

Fig. 2 depicts the rate coverage probability of both the SBSs operating in the IBFD mode and that are operating in the OBFD mode as a function of their corresponding fractions (i.e., $q\lambda_s'$ and $(1-q)\lambda_s'$, respectively). Simulation results validate the accuracy of the derived expressions and demonstrate that the impact of the considered mean load approximation (i.e., $\mathbb{E}[\mathcal{N}_s] = \lambda_s'/\lambda_c'$) on the gap between the simulation and analytical results is negligible. Note that the rate coverage of both kinds of SBSs (i.e., operating in IBFD and OBFD modes) tends to degrade with the increase in the corresponding proportion (i.e., q and $1-q$, respectively). This is due to the increased co-tier interference at their corresponding access links as the intensity of the interfering SBSs increases. This trend remains valid for any intensity of SBSs as can be seen for both $\lambda_s' = 50$ and $\lambda_s' = 100$ in Fig. 2(a) and (b), respectively.

Fig. 2 also shows the higher rate coverage of SBSs in IBFD mode when the intensity of SBSs (i.e., λ_s') is high. For example, at $\lambda_s' = 100$, 10% of IBFD SBSs in the network experience a much higher (70%) rate coverage compared to the case when $\lambda_s' = 50$. Moreover, comparing the rate coverage of 10% of SBSs in the IBFD mode and 10% of SBSs in the OBFD mode, it is observed that the IBFD SBSs outperform the OBFD SBSs. The underlying reason is that both the access and backhaul links of 10% IBFD SBSs do not experience any interference from the large proportion of OBFD SBSs. However, the backhaul links of 10% of OBFD SBSs are vulnerable to the interference caused by 90% of IBFD SBSs. In particular, due to the co-tier interference from the large proportion of IBFD SBSs, the OBFD SBSs may not enhance their rate coverage significantly even for low proportion of OBFD SBSs in the network.

Finally, Fig. 2 depicts that a small cell network of 100% IBFD SBSs or 100% OBFD SBSs may not be beneficial. Instead, an appropriate value of q can be selected that enhances either the overall rate coverage of a typical user or ensures a fair rate coverage at all SBSs in the network. For instance, when $\lambda_s' = 100$, a proportion of 70%-30% IBFD-OBFD SBSs in the network achieves a balanced rate coverage. On the other hand, when $\lambda_s' = 50$, a proportion of 45%-55% IBFD-OBFD SBSs achieves a balanced rate coverage.

B. Rate Coverage vs. Intensity of SBSs

Fig. 3 shows the downlink rate coverage of an IBFD and an OBFD SBS as a function of the intensity of SBSs in the network. In general, it can be seen that, for a given q, an increasing number of SBSs reduces the rate coverage of OBFD SBSs. This behavior is evident from the increasing co-tier interference at the access and backhaul links of OBFD SBSs. Although a CN cannot support more than $\mathcal{S}$ SBSs, the co-tier interference can continue to increase even when $\mathcal{N}_s$

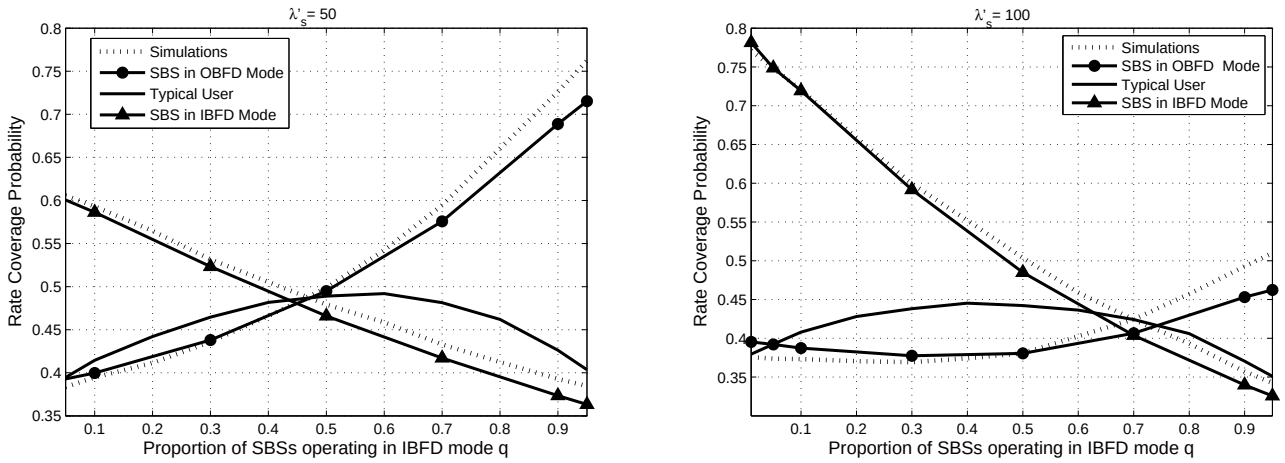

(a) (b)

Fig. 2: Rate coverage probability of SBSs operating in IBFD mode and OBFD mode as well as a typical user in the downlink as a function of the proportion of IBFD SBSs considering two different intensities of SBSs (for $\lambda'_c = 10$): (a) $\lambda'_s = 50$ and (b) $\lambda'_s = 100$.

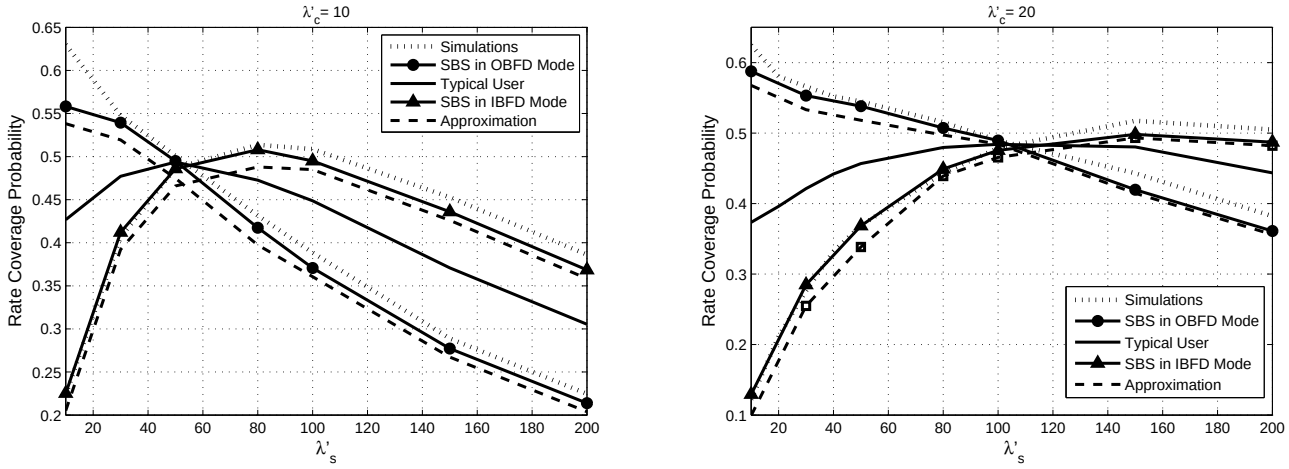

(a) (b)

Fig. 3: Rate coverage probability of SBSs operating in IBFD mode and OBFD mode as well as a typical user in the downlink as a function of the intensity of SBSs considering two different intensities of CNs (for $q = 0.5$): (a) $\lambda'_c = 10$ and (b) $\lambda'_c = 20$.

becomes greater than $\mathcal{S}$ since the distance of $\mathcal{S}$ selected SBSs can continue to reduce with the increase in λ'_s.

In contrast to OBFD SBSs, the rate coverage of an IBFD SBS is observed to increase first up to some point and then decrease as λ'_s increases. That is, for a given proportion q of IBFD SBSs, the number of SBSs in the network can be optimized to enhance the rate coverage of IBFD SBSs. An increase in the rate coverage is observed first due to relatively small backhaul interference incurred at a typical user. However, after a certain point, the backhaul interference becomes more significant and the rate coverage starts to decrease.

The trends remain same for different intensities of CNs. However, it can be observed from Fig. 3(b) that a high intensity of CNs is preferable for OBFD mode due to the possibility of strong backhaul links. On the other hand, an increased intensity of CNs yields a higher backhaul interference in IBFD mode. Consequently, as λ'_c increases, the optimal intensity of SBSs for IBFD mode also increases. It can thus be concluded that a high intensity of SBSs and CNs favours the IBFD mode and the OBFD mode, respectively.

C. Impact of SI Cancellation

Fig. 4 depicts the impact of increasing the SI cancellation on the performance of SBSs in IBFD mode. As expected, an increase in the SI cancellation increases the rate coverage of SBSs in IBFD mode whereas the performance of the SBSs in OBFD mode remains unchanged. For low intensities of SBSs in the network, a higher SI cancellation value may be required to achieve the rate coverage gains of IBFD over OBFD mode. This is because the weak access links (due to sparse and thus far-away SBSs) require high transmit power and consequently

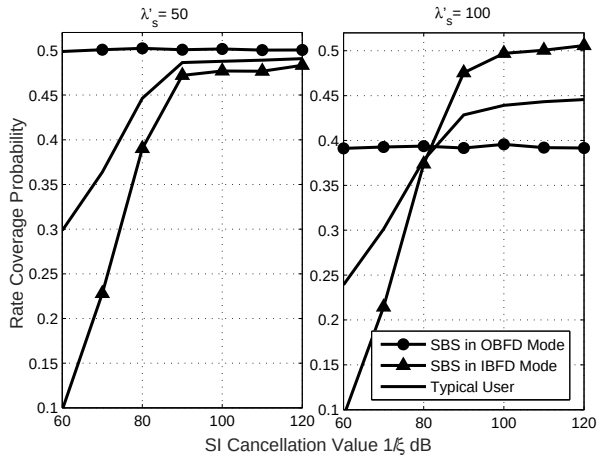

Fig. 4: Rate coverage probability of SBSs operating in IBFD mode and OBFD mode as well as a typical user in the downlink as a function of the SI cancellation value considering two different intensities of SBSs in the network (for $q = 0.5$, $\lambda'_c = 10$): (a) $\lambda'_s = 50$ and (b) $\lambda'_s = 100$.

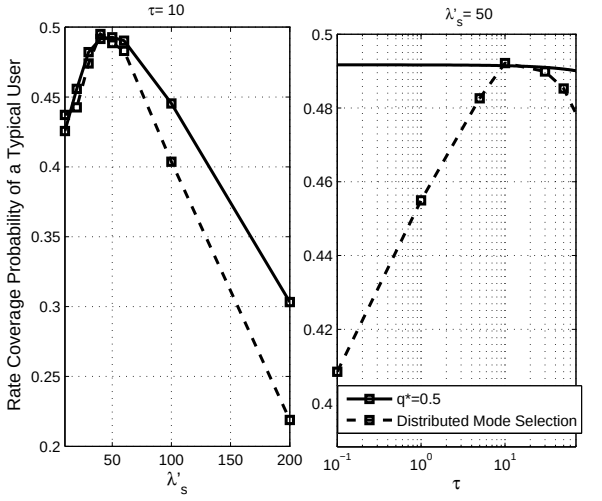

Fig. 5: Rate coverage probability of a typical user in the downlink with distributed mode selection (for $q^* = 0.5$, $\lambda'_c = 20$).

high SI cancellation is required at the SBSs to achieve high rate coverage. As such, in scenarios with low λ'_s, it may not be possible to achieve the gains of IBFD over OBFD mode as is also evident from Fig. 2 and Fig. 3. The OBFD-only mode will thus be the right-choice in such scenarios.

D. Distributed Mode Selection

Fig. 5 illustrates the impact of distributed mode selection on the rate coverage of a typical user. For comparison, we consider $q^* = 0.5$ which is the optimal proportion of IBFD and OBFD SBSs when $\lambda'_c = 10$ and $\lambda'_s = 50$ as shown in Fig. 2(a). It can be clearly observed that the optimal value of τ is 10 for $\lambda'_s = 50$. With this value, the distributed mode selection achieves near optimal performance at $\lambda'_s = 50$ and other low values of λ'_s. However, the threshold value $\tau = 10$ does not work optimally for higher values of λ'_s. The value of τ will therefore need to be optimized for different network parameters.

E. Backhaul Interference Mitigation

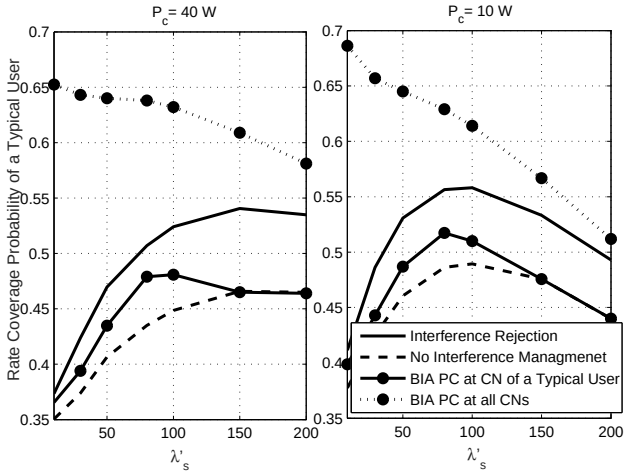
P_c = 40 W
P_c = 10 W
Rate Coverage Probability of a Typical User
λ'_s
Interference Rejection
No Interference Managmenet
BIA PC at CN of a Typical User
BIA PC at all CNs

Fig. 6: Rate coverage probability of a typical user with interference mitigation schemes implemented at IBFD SBSs considering two different CN's transmit power (for $q = 0.5$, $\lambda'_c = 20$).

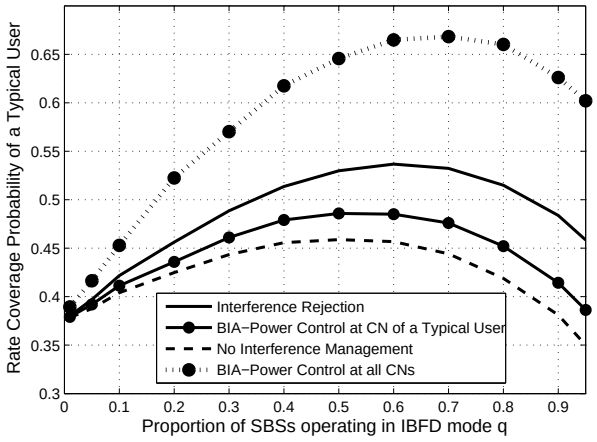
Rate Coverage Probability of a Typical User
Proportion of SBSs operating in IBFD mode q
Interference Rejection
BIA−Power Control at CN of a Typical User
No Interference Management
BIA−Power Control at all CNs

Fig. 7: Rate coverage probability of a typical user with interference mitigation schemes implemented at IBFD SBSs as a function of the proportion of IBFD and OBFD SBSs q.

Fig. 6 depicts the rate coverage of a typical user with interference mitigation schemes (i.e., interference rejection and BIA power control) considering different values of the CN's transmit power. As the available transmit power per CN increases, the gains of interference mitigation schemes become more evident. This is due to the fact that high transmit power leads to high backhaul interference, and therefore, the benefit of interference mitigation becomes more evident. It can also be observed that if the BIA power control scheme is applied only to the designated CN which is associated with the SBS of the typical user, significant gains can be achieved. In fact, for

low intensity of SBSs, the rate coverage becomes similar to that due to the interference rejection scheme. This is because the impact of backhaul interference from neighboring CNs is relatively low compared to the designated CN. However, for high intensity of SBSs, the gains are negligible due to the significant backhaul interference from neighboring CNs. Finally, it is observed that once the power control is applied by all CNs for their corresponding SBSs, the rate coverage of a typical user enhances significantly. The reason is the reduction in cross-tier interference from all neighboring CNs.

Fig. 7 quantifies the gain of implementing interference mitigation schemes at IBFD SBSs as a function of q. As expected, the higher the fraction of IBFD SBSs, the gains of interference mitigation become more evident. Also, the optimal value of q increases with interference mitigation due to the enhancement in IBFD mode.

F. Extensions to Include the Impact of Pilot Contamination

In order to include the impact of pilot contamination, we need to consider additional interference at the backhaul of all SBSs. The interference due to pilot contamination is received from those CNs that are reusing the same pilot sequences. The interfering CNs follow a thinned PPP of Φ_c and the intensity Φ_c can be given as mentioned below.

Assume that a set of $\mathcal{S}$ orthogonal pilot sequences is reused at each CN. In case where the number of associated SBSs at a given CN is less than the number of supported streams, i.e., $\mathcal{N}_s < \mathcal{S}$, the probability of the use of a pilot sequence at that CN and in turn receiving interference from that CN is $\frac{\mathcal{N}_s}{\mathcal{S}}$. Otherwise, all the pilot sequences will be reused at that CN; thus the probability of receiving interference from that CN is unity. The probability of receiving interference from a CN can thus be given as $\mathbb{P}(\mathcal{N}_s \geq \mathcal{S}) + \frac{\mathcal{N}_s}{\mathcal{S}}\mathbb{P}(\mathcal{N}_s < \mathcal{S})$. Consequently, the PPP of interfering CNs $\bar{\Phi}_{\rm c}$ with intensity $\bar{\lambda}_{\rm c}$ can be obtained by thinning the PPP Φ_c, i.e., $\bar{\lambda}_{\rm c} = \lambda_c \left(\mathbb{P}(\mathcal{N}_s \geq \mathcal{S}) + \frac{\mathcal{N}_s}{\mathcal{S}}\mathbb{P}(\mathcal{N}_s < \mathcal{S})\right)$. Since the PMF of $\mathcal{N}_s$ is given by (3), $\bar{\lambda}_{\rm c}$ can be given as follows:

$$\begin{aligned}\bar{\lambda}_{\rm c} &= \lambda_c \left(1 - \sum_{n=0}^{\mathcal{S}} \mathbb{P}(\mathcal{N}_s = n) + \sum_{n=0}^{\mathcal{S}} \frac{n}{\mathcal{S}} \mathbb{P}(\mathcal{N}_s = n)\right), \\ &= \lambda_c \left(1 - \sum_{n=0}^{\mathcal{S}} \left(1 - \frac{n}{\mathcal{S}}\right) \mathbb{P}(\mathcal{N}_s = n)\right). \end{aligned} \tag{45}$$

Consequently, the interference due to pilot contamination at IBFD and OBFD SBSs can be modeled as follows: [25, Appendix A]:

$$I_{\rm PC} = \sum_{y \in \bar{\Phi}_c \setminus {\rm c}} \frac{M - \min(\mathcal{N}_s, \mathcal{S}) + 1}{\min(\mathcal{N}_s, \mathcal{S})} P_c r_{\rm y,s}^{-\beta}. \tag{46}$$

The Laplace transform of $I_{\rm PC}$ and in turn the rate coverage probability analysis can be conducted using tools similar to those used in Section IV.

VIII. Conclusion

We have investigated the performance of a massive MIMO-enabled wireless backhaul network which is composed of a mixture of small cells configured either in the in-band or out-of-band FD backhaul mode. Downlink coverage probability has been derived for a typical user considering both the IBFD and OBFD modes. Closed-form expressions have been provided for special cases. Under perfect backhaul assumption, a closed-form expression of the optimal proportion of IBFD and OBFD SBSs has been derived. It has been shown that selecting a correct proportion of out-of-band small cells in the network is crucial in obtaining a high rate coverage. Also, selecting an appropriate SI cancellation value is also crucial to achieve the gains of IBFD over OBFD mode. The impact of various sources of interferences at the access and backhaul links of SBSs has been investigated and few remedial solutions for backhaul interference management have been presented. The significance of the backhaul interference mitigation is found to be more evident in scenarios with high transmit power of CNs and low intensity of SBS. The framework can be extended to include multiple antennas at SBSs, to consider the possibility of serving users through CNs, i.e., depending on the coverage requirements a user can opportunistically switch between SBSs and CNs. Moreover, the problem of optimal partitioning of a spectrum band for non-overlapping deployment of IBFD and OBFD SBSs (i.e., deployment across different sub-bands) can be investigated.

References

[1] E. Hossain, M. Rasti, H. Tabassum, and A. Abdelnasser, "Evolution toward 5G multi-tier cellular wireless networks: An interference management perspective," *IEEE Wireless Communications*, vol. 21, no. 3, pp. 118–127, June 2014.

[2] U. Siddique, H. Tabassum, E. Hossain, and D. Kim, "Wireless backhauling of 5g small cells: challenges and solution approaches," *Wireless Communications, IEEE*, vol. 22, no. 5, pp. 22–31, 2015.

[3] X. Ge, H. Cheng, M. Guizani, and T. Han, "5G wireless backhaul networks: Challenges and research advances," *IEEE Transactions on Communications*, vol. 28, no. 6, pp. 6–11, Nov. 2014.

[4] G.-P. Liu, R. Yu, H. Ji, V. Leung, and X. Li, "In-band full-duplex relaying: A survey, research issues and challenges," *IEEE Communications Surveys and Tutorials, to appear*, Jan. 2015.

[5] K. M. Thilina, H. Tabassum, E. Hossain, and D. I. Kim, "Medium access control design for full-duplex wireless systems: Challenges and approaches," *IEEE Communications Magazine*, vol. 53, no. 5, pp. 112–120, May 2015.

[6] M. Duarte, A. Sabharwal, V. Aggarwal, R. Jana, K. K. Ramakrishnan, C. W. Rice, and N. K. Shankaranarayanan, "Design and characterization of a full-duplex multiantenna system for WiFi networks," *IEEE Transactions on Vehicular Technology*, vol. 63, no. 3, pp. 1160–1177, Mar. 2014.

[7] S. Samarakoon, M. Bennis, W. Saad, and M. Latva-aho, "Backhaul-aware interference management in the uplink of wireless small cell networks," *IEEE Transactions on Communications*, vol. 12, no. 11, pp. 5813–5825, Nov. 2013.

[8] N. Wang, E. Hossain, and V. K. Bhargava, "Joint downlink cell association and bandwidth allocation for wireless backhauling in two-tier HetNets with large-scale antenna arrays," *arXiv:1501.00078v1*, 2015.

[9] J. Zhao, T. Q. S. Quek, and Z. Lei, "Heterogeneous cellular networks using wireless backhaul: Fast admission control and large system analysis," *arXiv:1501.06988v1*, Jan. 2015.

[10] S. Goyal, L. Pei, S. Panwar, R.A. DiFazio, Y. Rui, L. Jialing, and E. Bala, "Improving small cell capacity with common-carrier full duplex radios," *in Proc. of IEEE International Conference on Communications (ICC'14)*, pp. 4987–4993, June 2014.

[11] J. Yun, "Intra and inter-cell resource management in full-duplex heterogeneous cellular networks," *IEEE Transactions on Mobile Computing, to appear*, Apr. 2015.

[12] C. Nam, C. Joo, and B. S., "Joint subcarrier assignment and power allocation in full-duplex OFDMA networks," *IEEE Transactions on Wireless Communications*, vol. 14, no. 6, pp. 3108–3119, June 2015.

[13] J. Lee and T. Q. Quek, "Hybrid full-/half-duplex system analysis in heterogeneous wireless networks," *IEEE Transactions on Wireless Communications*, vol. 14, no. 5, pp. 2883–2895, Jan. 2015.
[14] O. Simeone, E. Erkip, and S. Shamai, "Full-duplex cloud radio access networks: An information-theoretic viewpoint," *IEEE Wireless Communications Letters*, vol. 3, no. 4, pp. 413–416, Aug. 2014.
[15] S. Barghi, A. Khojastepour, K. Sundaresan, and S. Rangarajan, "Characterizing the throughput gain of single cell MIMO wireless systems with full duplex radios," *in Proc. of 10th International Symposium on Modeling and Optimization in Mobile, Ad Hoc and Wireless Networks (WiOpt'12)* , pp. 68–74, May 2012.
[16] B. Li and P. Liang, "Small cell in-band wireless backhaul in massive MIMO systems: A cooperation of next-generation techniques," *arXiv:1402.2603*, 2014.
[17] S. Gradshteyn and I. M. Ryzhik, *Table of Integrals, Series, and Products*. 6th edition, New York: Academic Press, 2000.
[18] H. ElSawy, E. Hossain, and M. Haenggi, "Stochastic geometry for modeling, analysis, and design of multi-tier and cognitive cellular wireless networks: A survey," *Communications Surveys and Tutorials, IEEE*, vol. 15, no. 3, pp. 996–1019.
[19] S. Al-Ahmadi and H. Yanikomeroglu, "On the approximation of the generalized-K distribution by a gamma distribution for modeling composite fading channels," *IEEE Transactions on Wireless Communications*, vol. 9, no. 2, pp. 706–713, Feb. 2010.
[20] H. Dhillon and J. Andrews, "Downlink rate distribution in heterogeneous cellular networks under generalized cell selection," *IEEE Wireless Communications Letters*, vol. 3, no. 1, pp. 42–45, Feb. 2014.
[21] D. Bethanabhotla, O. Y. Bursalioglu, H. C. Papadopoulos, and G. Caire, "User association and load balancing for cellular massive MIMO," pp. 1–10, 2014.
[22] T. L. Marzetta, "Noncooperative cellular wireless with unlimited numbers of base station antennas," *IEEE Transactions on Wireless Communications*, vol. 9, no. 11, pp. 3590–3600, 2010.
[23] A. H. Sakr and E. Hossain, "Cognitive and energy harvesting-based D2D communication in cellular networks: Stochastic geometry modeling and analysis," *IEEE Transactions on Communications*, vol. 63, no. 5, pp. 1867–1880, Mar. 2015.
[24] A. Erdelyi, W. Magnus, F. Oberhettinger, and F. G. Tricomi, *Higher Transcendental Functions – Vol I*, 6th ed. New York, NY, USA: McGraw-Hill, 1953.
[25] D. Bethanabhotla, O. Bursalioglu, H. Papadopoulos, and G. Caire, "Optimal user-cell association for massive mimo wireless networks," *IEEE Transactions on Wireless Communications, Early Access Articles*, Nov. 2015.